Atmos. Chem. Phys., 11, 1813–1835, 2011
www.atmos-chem-phys.net/11/1813/2011/
doi:10.5194/acp-11-1813-2011

Atmospheric Chemistry and Physics

Influence of meteorology on PM_{10} trends and variability in Switzerland from 1991 to 2008

I. Barmpadimos[1], C. Hueglin[2], J. Keller[1], S. Henne[2], and A. S. H. Prévôt[1]

[1]Paul Scherrer Institute, Villigen, Switzerland
[2]Swiss Federal Laboratories for Material Science and Technology, Dübendorf, Switzerland

Received: 16 September 2010 – Published in Atmos. Chem. Phys. Discuss.: 9 November 2010
Revised: 28 January 2011 – Accepted: 10 February 2011 – Published: 28 February 2011

Abstract. Measurements of airborne particles with aerodynamic diameter of 10 µm or less (PM_{10}) and meteorological observations are available from 13 stations distributed throughout Switzerland and representing different site types. The effect of all available meteorological variables on PM_{10} concentrations was estimated using Generalized Additive Models. Data from each season were treated separately. The most important variables affecting PM_{10} concentrations in winter, autumn and spring were wind gust, the precipitation rate of the previous day, the precipitation rate of the current day and the boundary layer depth. In summer, the most important variables were wind gust, Julian day and afternoon temperature. In addition, temperature was important in winter. A "weekend effect" was identified due to the selection of variable "day of the week" for some stations. Thursday contributes to an increase of 13% whereas Sunday contributes to a reduction of 12% of PM_{10} concentrations compared to Monday on average over 9 stations for the yearly data. The estimated effects of meteorological variables were removed from the measured PM_{10} values to obtain the PM_{10} variability and trends due to other factors and processes, mainly PM_{10} emissions and formation of secondary PM_{10} due to trace gas emissions. After applying this process, the PM_{10} variability was much lower, especially in winter where the ratio of adjusted over measured mean squared error was 0.27 on average over all considered sites. Moreover, PM_{10} trends in winter were more negative after the adjustment for meteorology and they ranged between $-1.25\,\mu g\,m^{-3}\,yr^{-1}$ and $0.07\,\mu g\,m^{-3}\,yr^{-1}$. The adjusted trends for the other seasons ranged between $-1.34\,\mu g\,m^{-3}\,yr^{-1}$ and $-0.26\,\mu g\,m^{-3}\,yr^{-1}$ in spring, $-1.40\,\mu g\,m^{-3}\,yr^{-1}$ and $-0.28\,\mu g\,m^{-3}\,yr^{-1}$ in summer and $-1.28\,\mu g\,m^{-3}\,yr^{-1}$ and $-0.11\,\mu g\,m^{-3}\,yr^{-1}$ in autumn. The estimated trends of meteorologically adjusted PM_{10} were in general non-linear. The two urban street sites considered in the study, Bern and Lausanne, experienced the largest reduction in measured and adjusted PM_{10} concentrations. This indicates a verifiable effect of traffic emission reduction strategies implemented during the past two decades. The average adjusted yearly trends for rural, urban background and urban street stations were -0.37, -0.53 and $-1.2\,\mu g\,m^{-3}\,yr^{-1}$ respectively. The adjusted yearly trends for all stations range from $-0.15\,\mu g\,m^{-3}\,yr^{-1}$ to $-1.2\,\mu g\,m^{-3}\,yr^{-1}$ or $-1.2\%\,yr^{-1}$ to $-3.3\%\,yr^{-1}$.

1 Introduction

Airborne particles with aerodynamic diameter of 10 µm or less (PM_{10}) have important negative consequences on human health (Zemp et al., 1999; Bayer-Oglesby et al., 2005). International organizations and governments worldwide have tried to reduce emissions and human exposure to PM_{10} by issuing guidelines and directives and by taking a number of legislative measures. In Switzerland yearly average PM_{10} concentrations should not exceed $20\,\mu g\,m^{-3}$ and a daily average value of $50\,\mu g\,m^{-3}$ should not be exceeded more than once a year (Swiss Federal Council, 2010a). As of 2008 the European Union has introduced legislation for $PM_{2.5}$ as well (European Parliament and the Council, 2008). As a result of the implementation of air quality legislation, air pollution levels (including particulate matter) in most developed countries have declined after 1970 (Darlington et al., 1997). Further implementation and assessment of mitigation policies require high quality long-term datasets providing quantitative air quality information at a regional level. When such datasets exist, a detailed investigation of PM_{10} trends is of great value both on a scientific and on a regulatory level.

An important aspect to be considered when studying trends of air pollution is that the trends do not only depend on the emissions of certain pollutants but also on the

Correspondence to: A. S. H. Prévôt
(andre.prevot@psi.ch)

meteorological conditions in the area of interest (Gomiscek et al., 2004). Hooyberghs et al. (2005) reported in a study for Belgian urban centers that day-to-day PM_{10} concentrations depend more on meteorology than on anthropogenic emissions. Pryor and Barthelmie (1996) emphasized that, one should first isolate and remove the effect of weather conditions before investigating the influence of anthropogenic activities on air pollution. To do so, knowledge of the dependence of the concentrations of certain pollutants on various meteorological variables is required. Only a few studies exist on this wide research field. For example, Easter and Peters (1994) demonstrated the non-linear effect of temperature and relative humidity changes on sulphate aerosol. However, temperature and relative humidity represent only a few of the meteorological variables that affect pollutant concentrations.

Although this study does not focus on PM_{10} chemical composition, it is important to acknowledge that PM_{10} is a complex mixture of chemical compounds whose behaviour depends strongly on the atmospheric conditions. In a paper that summarises data from a number of European sites, Putaud et al. (2004) report that for the four Swiss sites included in their study (Bern, Zurich, Basel and Chaumont), the most important compounds in terms of their contribution to total PM_{10} mass are black carbon, organic matter, mineral dust, ammonium, nitrate and sulphate, while a considerable unaccounted fraction is present as well. The relative contribution of different species to the total PM_{10} mass varies between different site types. The kerbside site at Bern has a relatively large fraction of black carbon and a low fraction of sulphate and ammonium. Mineral dust fraction was large at the kerbside station and at the rural station at Chaumont whereas it was low at the urban background stations at Zurich and Basel. Ammonia and nitrate have the largest fraction at urban background sites and a low fraction at the rural site. Further important consituents of PM_{10} in Switzerland are organic matter and the unaccounted fraction which do not vary significantly between different site types and seasons. Information on the chemical composition of organic aerosol for different sites is given by Lanz et al. (2010), who show that the oxygenated secondary fraction is the dominating organic fraction. For PM_1 in general, larger differences are found between the seasons compared to station types. A further chemical characterisation of PM_{10} at Swiss sites including water soluble ions and trace elements is found in Hueglin et al. (2005).

Several methodologies for modeling of PM_{10} trends and for prediction of PM_{10} concentrations are reported in the literature. Zolghadri and Cazaurang (2006) developed an adaptive nonlinear model for the prediction of PM_{10} in the Bordeaux area. However, the methodology for the development of the model has strong empirical elements, which make it strictly valid only for the area that it was developed for. Another approach for statistical modeling of PM_{10} involves neural networks (Hooyberghs et al., 2005), which demonstrated a fairly good predictive skill of PM_{10} for Belgium. Ordóñez et al. (2005) used an extensive meteorological dataset to carry out a statistical analysis of the effect of weather on ozone trends in Switzerland (see also Keller et al., 2008). In this study however, it was assumed that ozone has a linear dependence on each meteorological variable. In a more recent analysis of the effect of meteorology on PM_{10} trends in the Netherlands (Velders and Matthijsen, 2009) it was assumed that the long term trend was only a result of emissions and that meteorology only affects the variability of PM_{10} concentrations after removing the trends. However, it is shown later that changes in meteorology can also be responsible for long term changes in PM_{10} concentrations.

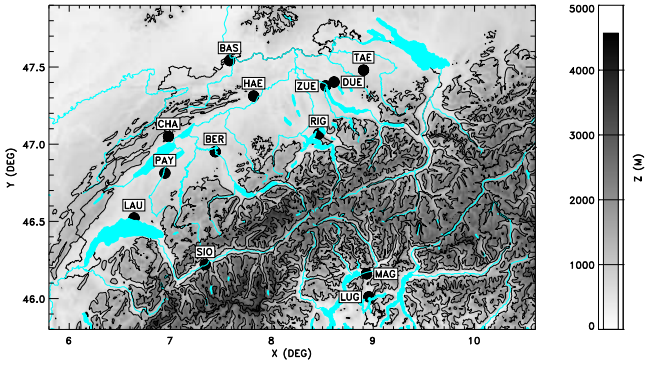

Fig. 1. Location of the stations used in the analysis. See correspondence between station codes and names in Table 1. Sidebar indicates height above mean seal level.

To carry out an adequate investigation of PM_{10} trends, one needs a good spatial and temporal coverage of the region in question (Pryor and Barthelmie, 1996). PM_{10} measurements within the Swiss National Air Pollution Monitoring Network (NABEL) are available from 13 stations since 1991, providing a rare opportunity to study the PM_{10} trends during a time period with marked changes in air pollution levels in developed countries. The stations represent various site types and altitudes (see Table 1). Details on the dataset used in this study are given in Sect. 2. The effect of a range of available meteorological variables on PM_{10} was estimated by Generalized Additive Models (GAMs). PM_{10} trends in each season were investigated separately. A description of the methodology is found in Sect. 3. The results and the conclusions are presented in Sects. 4 and 5 respectively.

2 Data

PM_{10} concentrations used in this study were measured at 13 sites of the Swiss National Air Pollution Monitoring Network NABEL (Empa, 2010). The names and details of the considered sites are listed in Table 1 and their locations are shown in Fig. 1.

Table 1. Stations used in the analysis. The PM_{10} concentrations correspond to the mean daily value of all available data. See Table 5 for the periods of available data for each station.

Station code	Station name	Altitude (m a.s.l.)	Station type	Mean PM_{10} ($\mu g\,m^{-3}$)
BAS	Basel	365	suburban	25.9
BER	Bern	596	urban/street	39.0
CHA	Chaumont	1187	rural mountain	12.9
DUE	Dübendorf	480	suburban	25.4
HAE	Härkingen	479	rural/highway	29.0
LAU	Lausanne	577	urban/street	33.7
LUG	Lugano	332	urban/background	34.7
MAG	Magadino	254	rural lowland	31.5
PAY	Payerne	539	rural lowland	23.2
RIG	Rigi	1079	rural mountain	13.4
SIO	Sion	535	rural/highway	27.4
TAE	Tänikon	586	rural lowland	22.0
ZUE	Zürich	457	urban/background	27.0

The PM_{10} data were obtained using high-volume samplers (DHA-80, Digitel) and gravimetric determination of the collected PM mass. From 1991 until the end of 2005 glass fiber filters (Ederol 227/1/60) were used. Since then PM_{10} is collected on quartz fiber filters (Whatman QMA). Until 1997 the high volume samplers were equipped with inlets for total suspended particles (TSP). The TSP values from 1991 to 1997 were converted into PM_{10} by applying a factor that was derived separately for all site types during one year parallel PM_{10} measurements. For 1997, this factor is 0.63 for the urban kerbside site in Bern and between 0.81 and 0.90 for the other stations (Empa, 2010). The correction process for the TSP data ensures continuity of the TSP and PM_{10} timeseries. The main assumption involved in this correction is that the PM_{10} to TSP ratio at each station was approximately constant throught the 1991–1997 period and equal to the 1997 value. This is considered to be reasonable. Scatterplots of TSP measurements before and after scaling versus parallel PM_{10} measurements for year 1997 and for 8 stations are provided as supplementary material.

In 2001, the frequency of PM_{10} sampling for the gravimetric method was reduced from daily sampling to PM_{10} collection every fourth day. Since then, the gravimetric PM_{10} measurements are complemented by beta attenuation monitors (FH62-IR, Thermo ESM Andersen) and later on by TEOM FDMS (Thermo Environmental) instruments. However, the PM_{10} data obtained with the PM_{10} monitors were corrected to be consistent with gravimetrically determined PM_{10} for the days where gravimetrically determined PM_{10} were not available. The correction takes into account the previous and next gravimetric PM_{10} observation using the formula put forward by Gehrig et al. (2005). The correction of the beta monitor and TEOM data introduces some random noise but no bias and therefore no breaks or inconsistencies in the PM_{10} timeseries are caused by the change of the sampling period from 1 to 4 days. The observational errors of the aforementioned measurement methods at the 95% level of confidence are 1.2 $\mu g\,m^{-3}$ for the gravimetric method, 1.4 $\mu g\,m^{-3}$ for the beta monitor and 2.2 $\mu g\,m^{-3}$ for the TEOM instrument.

At some of the sites meteorological measurements are available from the NABEL network. The remaining sites are collocated with meteorological measurements stations operated by the Swiss weather service (MeteoSwiss) and meteorological data were provided from MeteoSwiss. The meteorological data measured include wind speed, wind direction, precipitation, global radiation, net radiation, air temperature and relative humidity. NABEL and MeteoSwiss use the same instruments for their meteorological measurements.

Wind speed and wind direction are measured using a rotating cup anemometer and a weather vane located typically at 10 m above ground. Precipitation is measured by means of a tipping bucket rain gauge with a built-in heating system for measuring snow and ice. Further instrumentation installed at the sites includes a pyranometer for measuring global radiation and a pyranometer-pyrgeometer coupled system for the measurement of net radiation. Temperature is measured using a thermocouple and dewpoint is measured by a chilled mirror hygrometer. A detailed description of the instrumental setup for meteorology measurements is given in Empa (2010).

The resulting air pollution and meteorology datasets go through an automatic and manual evaluation to ensure that certain criteria are fulfilled. Namely, the data should be within a plausible range as well as showing plausible variability. Moreover, the data should reproduce to a reasonable extent the expected daily, monthly and yearly variations. Certain measured quantities which are related to each other are checked for consistency. Whenever possible, NABEL measurements are compared to nearby or similar stations with the expectation of similar values.

In addition to the daily average, the afternoon average of temperature, global irradiance, water mixing ratio and wind speed are calculated and used as meteorological variables as well. "Afternoon" values are the result of averaging hourly values between 12:00 and 18:00 (UTC+1). Such variables are hereafter denoted with the letter "a" at the beginning of their name. Averages for the morning (06:00–12:00 UTC+1) and evening (18:00–24:00 UTC+1) periods were calculated as well. These are denoted with "m" and "e" respectively.

Wind speed measurements were complemented by calculating wind gust. The maximum wind speed values of 10-min intervals were recorded and the resulting six values every hour were averaged to obtain hourly wind gust. A further 24-h averaging was done to obtain the daily data.

It is known that the atmospheric boundary layer height and the strength of the temperature inversion at the top of the boundary layer play an important role in determining the levels of PM_{10} by mixing and deposition mechanisms. As a proxy for the vertical gradient of the potential temperature, the difference of an approximate potential temperature between two nearby meteorological stations with large altitude difference was used (Ordóñez et al., 2005). Different pairs of stations were used for the areas north of the Alps (Swiss Plateau) and south of the Alps. A further measure of the vertical mixing in the boundary layer is the convective available potential energy (CAPE) which is estimated using meteorological soundings from the rural station at Payerne. A simple parcel method as described in Seibert et al. (2000) with a surface excess temperature of 0.1 K was used to calculate convective boundary layer depths from the same soundings.

A relationship between the transatlantic transport of ozone and the North Atlantic Oscillation (NAO) index has been demonstrated in the last few years in the literature (Creilson et al., 2003; Eckhardt et al., 2003). In order to investigate a possible influence on PM_{10} concentrations in Switzerland, a monthly station-based NAO index (Jones et al., 1997) was used in the analysis.

The categorical variable "synoptic group" as calculated in the Alpine Weather Statistics AWS (Wanner et al., 1998) was used for representation of the impact of the general synoptic weather conditions on PM_{10} in Switzerland. Moreover, variables "front" and "days since front" from the AWS were also included in this trend analysis to account for a possible current or past presence of a frontal passage. Another variable which records the history of the weather conditions is the amount of precipitation on the previous day, denoted here as "yesterday precipitation". Further details on the meteorological variables which were constructed and used in this study can be found in Ordóñez et al. (2005). For each station and season, only those meteorological variables with less than 30% missing values were included in the data analysis procedure described below.

3 Statistical method

3.1 Description of the statistical model

In order to properly investigate the relationship between PM_{10} concentrations and meteorological variables one has to consider that these relationships can be non-linear. A way to model such non-linear relationships is to use Generalized Additive Models GAMs (Hastie and Tibshirani, 1990; Wood, 2006). GAM models were constructed for each station and season separately for the period from 1991–2008. For comparison purposes GAMs were run for the yearly data of all stations as well. All calculations were carried out using the statistical software R (R Development Core Team, 2008). The process yielded a total of 65 GAMs. The general formula of these models reads:

$$\ln PM_{10} = a + s_1(A_1) + s_2(A_2) + \ldots + b_{11}B_{11} + b_{12}B_{12} + \ldots + b_{21}B_{21} + b_{22}B_{22} + \ldots + \varepsilon \quad (1)$$

where a: intercept

$s_1(A_1) + s_2(A_2) + \ldots$: smooth functions s_i of continuous covariates A_i

$b_{11}B_{11} + b_{12}B_{12} + \ldots + b_{21}B_{21} + b_{22}B_{22} + \ldots$: B_{ij} denote categorical variables. Index i denotes the kind of categorical variable (e.g. synoptic group, front, day of the week etc.) and index j denotes the category. For example, categorical variable synoptic group has eight possible categories each one representing a different synoptic group. Therefore, if synoptic group is denoted by B_{1j}, then B_{1j} has eight possible values ranging from B_{11} to B_{18}. B_{ij} is equal to 1 when the day in question is classified under category B_{ij} and 0 otherwise. b_{ij} is the corresponding coefficient.

ε: error term

A logarithmic link function was deemed suitable for GAMs in (1) because it improved the characteristics of the model residuals (see Sect. 3.2).

Functions s_i are thin plate regression splines (see Wood, 2008 and references therein), which were estimated using the mgcv library of R. These functions are the result of a minimization procedure where smoothness is ensured by an appropriately selected penalization term. However, unlike a full thin plate spline, the basis is truncated to obtain a low rank smoother which is relatively fast to compute.

GAMs can be applied to a wide variety of data sets independently of location (including atmospheric data) under the assumption that the target variable has an additive relationship to the explanatory variables.

3.2 Model selection

A forward elimination procedure was used for the selection of the model covariates. This procedure is a modified version of the variable selection process put forward by Jackson et al. (2009). The employed algorithm includes the following 6 steps:

Step 1 – The first variable was selected: All available explanatory variables were substituted one after the other into the model to construct GAMs with one variable. A version of the Akaike Information Criterion AIC (Akaike, 1974) was calculated for each model and the GAM with the lowest AIC was selected (see Eq. 3 for definition of AIC).

Step 2 – The next variable was added: The remaining explanatory variables were substituted to the existing model one after the other. The GAM with the lowest AIC was selected.

Step 3 – The choice from the first step was confirmed: The variable which was chosen in the first step was removed and each one of the remaining variables was added to the model. If this processes resulted in a model with lower AIC than the model selected in step 2, then the model from the current step was chosen.

Step 4 – Collinearity was tested: Collinearity occurs when two model covariates have a linear relationship. This makes the individual contribution of each variable difficult to discern, introduces redundancy and makes the model excessively sensitive to the data (Jackson et al., 2009). The Variance Inflation Factor VIF (Freund and Wilson, 1998) was calculated as a measure of collinearity of each covariate with each one of the other variables in the model. VIF was calculated according to the relationship

$$\mathrm{VIF} = \frac{1}{1 - R_j^2} \tag{2}$$

where R_j^2 is the coefficient of determination of the linear regression of the j-th variable in the model against the other variables. If a value of VIF = 2.5 was exceeded for a pair of covariates, the covariate whose addition to the model caused the smaller decrease of AIC was removed. The threshold of 2.5 for VIF corresponds to a coefficient of determination of 0.6 which was considered to represent a maximum acceptable degree of collinearity. Other, typically less strict cut-off values for VIF can be found in the literature. Montgomery and Peck (1992) suggest VIF = 5 and Kutner et al. (2004) suggest VIF = 10.

Step 5 – Steps 2 to 4 repeated: The aforementioned steps were repeated until the addition of an extra covariate resulted in an increase of AIC.

Step 6 – Julian day was added to the model: The PM_{10} values do not only depend on weather conditions but also on a number of different processes, which were not included in the model such as emissions of PM_{10} and precursors of secondary PM_{10}. One additional covariate, the time variable Julian Day (here defined as the number of days since 1 January 1960) was included in the pool of available covariates to capture PM_{10} variations due to any processes which were not explicitly accounted for. If this variable was not automatically selected in steps 1–5 of the variable selection algorithm, it was forcibly added in the end as an extra linear term. This was necessary as non-inclusion of this variable would return models whose error term instead of being random would potentially contain some interannual structure.

As a final step, it was checked that the residuals of the selected model fulfilled the criteria of normality, linearity and homoscedasticity (Wilks, 2006).

AIC was estimated using the relationship

$$\mathrm{AIC} = -2 \cdot \log L + k \cdot \mathrm{edf} \tag{3}$$

where

L: the maximized value of the likelihood function for the estimated model

edf: effective degrees of freedom of the model

k: the penalty parameter

Details on the calculation of AIC for GAMs can be found in Tibshirani et al. (1990) and Wood (2008). The second term on the right-hand side of Eq. (3) represents the severity of model penalization. Using the value $k = 24$ for the parameter k yields the classic AIC (Akaike, 1974) whereas $k = \log(n)$, n being the number of observations, yields the Bayesian Information Criterion BIC (Schwarz, 1978), which penalizes additional model terms more heavily. Nevertheless, both the use of AIC and BIC resulted in models with too many variables. A value of $k = 15$ was chosen here to sufficiently limit the number of selected variables in the models.

A similar model selection algorithm was used in Jackson et al. (2009). In that study however, the selection of the best model in each step of the algorithm was not based on AIC, but on deviance explained. The advantage of using the AIC in the model selection process is that, unlike simple use of deviance explained, the effective degrees of freedom of the model are taken into account. The effective degrees of freedom of a regression spline increase as wiggliness of the spline increases. Hence, using relationship (3) in the model selection process does not only control the number of variables in the model but also the wiggliness of the variables

to be selected. This method has the disadvantage that it usually yields GAMs with lower deviance explained because the model with lowest AIC chosen in each step of the algorithm does not necessarily coincide with the model with the highest deviance explained. It was deemed however appropriate to choose a methodology which results in models with conceptually more robust behavior.

3.3 Adjustment of PM_{10} concentrations for the effect of meteorology

Once the GAMs were constructed, PM_{10} values for the period in question were adjusted for meteorology (i.e. the effect of meteorology was removed). The adjusted PM_{10} values are the model estimates of the contribution of the Julian day plus the model intercept and the random model error. This reads:

$$\ln PM_{10\,\mathrm{adj}} = a + s(\text{Julian day}) + \varepsilon \quad (4)$$

The adjusted PM_{10} values include PM_{10} variability that is not the result of meteorology but of other factors such as the anthropogenic emissions.

To evaluate the model performance, all GAMs were developed using a random sample of 90% of the available observations. The remaining 10% of the observations of the explanatory variables were then substituted into the produced models to obtain modeled PM_{10} concentrations. These were then compared with the corresponding PM_{10} measurements (Sect. 4.4).

4 Results and discussion

4.1 Important explanatory variables and their relationship to PM_{10}

As shown in Eq. (1), the contribution of each explanatory variable to the logarithm of PM_{10} was calculated as an additive factor. Exponentiation of (1) yields a relationship between PM_{10} concentrations and the selected explanatory variables which are then expressed as multiplicative factors (hereafter referred to as "PM_{10} factors"), which contribute to an increase of PM_{10} if they are greater than 1 and a decrease of PM_{10} if they are less than 1. In this section the relationship between PM_{10} concentrations and each one of these estimated factors is presented. The exponentiated output was preferred because presenting the results in terms of PM_{10} concentrations was deemed more intuitive than a presentation in terms of the logarithm of PM_{10}.

Table 2 shows the frequency of occurrence of each explanatory variable in the GAMs corresponding to all 13 stations for each season and the whole year. A significant part of the available explanatory variables were chosen either infrequently or never. That is because they either did not have a firm relationship to PM_{10} or because other variables with a similar relationship to PM_{10} were preferred in the model selection process.

Table 2. Number of stations (out of 13) at which each variable was selected for each season and the whole year. Numbers in bold indicate that the variable was selected for more than half of the stations whereas numbers in italic indicate that the variable was selected for 4, 5 or 6 of the stations. Only the occurrences of Julian day which resulted from automatic selection are included in this table. Eventually, Julian day was added also in the models where it was initially not selected.

Variable/Definition	MAM	JJA	SON	DJF	Year
day of the week	3	4	3	1	**9**
Julian day	*5*	**13**	*5*	2	**12**
wind speed	0	2	0	0	0
wind gust	**12**	**11**	**12**	**12**	**12**
surface pressure	*4*	2	*4*	3	*5*
global irradiance	1	0	1	3	3
net irradiance	**7**	3	*4*	**7**	*4*
daily precipitation	**7**	3	**10**	**7**	**13**
relative humidity	**8**	4	4	3	*5*
temperature	1	*4*	2	**8**	**7**
water vapor mixing ratio	1	3	1	3	*4*
daily sunshine duration	*4*	1	1	2	0
convective available potential energy	3	4	2	3	2
afternoon global irradiance	1	4	*4*	1	*4*
afternoon temperature	1	**8**	2	0	0
afternoon mixing ratio	2	2	0	1	2
afternoon wind speed	1	2	0	0	0
afternoon sunshine duration	1	0	1	0	1
lightning great distance	0	0	3	0	1
lightning at small distance	1	0	3	0	3
convective boundary layer depth	**11**	2	**10**	**10**	**11**
NAO index	0	1	0	0	0
amount of precipitation the previous day	**9**	4	**8**	**8**	**12**
morning wind speed	2	1	1	1	2
morning global irradiance	3	1	0	1	3
morning sunshine duration	1	2	2	0	1
synoptic group	0	0	0	0	*4*
front	3	0	2	*4*	2
number of days since front	*5*	0	*6*	*4*	**11**
vertical gradient of potential temperature	2	2	*5*	*5*	*5*
lightning at afternoon and evening	0	0	0	0	1

The time variable "weekday" was only chosen once in winter whereas it was more frequently selected in summer, autumn and spring (4, 3 and 3 times respectively). All of the stations where weekday was selected are urban/street or rural/highway stations, which are more strongly affected by traffic emissions. Figure 2 shows the PM_{10} factor of the "day of the week" variable along with the standard error estimates at all stations where it was selected for summer.

These PM_{10} factors are expressed relative to the effect of Monday, which is taken as equal to unity. Therefore, there is no standard error for Monday. Note the increasing tendency of the influence on PM_{10} during the weekdays. The maximum influence occurs on Thursday which contributes to an increase of 9% on PM_{10} concentrations compared to Monday on average over the 4 stations shown in Fig. 2 for summer. Sunday contributes to a decrease of 17% compared to Monday for the same stations. "Day of the week" was selected 9 times for the yearly data and exhibited a similar weekly variation. Thursday contributes to an increase of 13% and

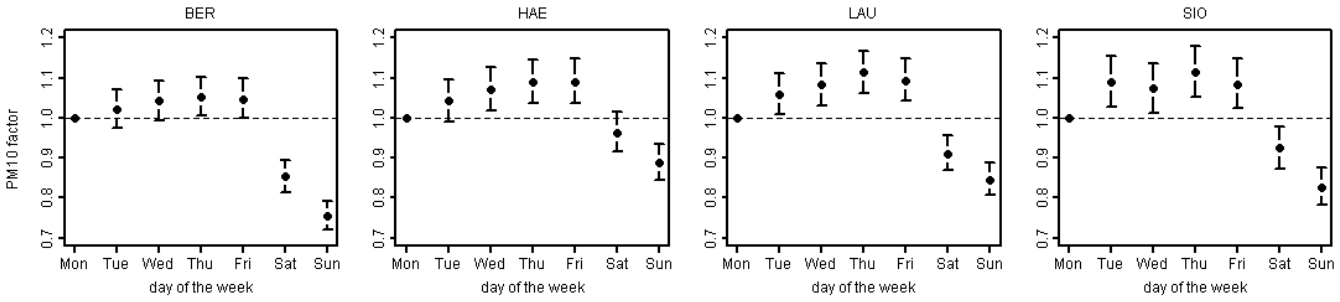

Fig. 2. The PM_{10} factor for the "day of the week" variable for summer. All factors have been divided by the Monday factor. The error bars indicate two standard errors. The influence of the day of the week was similar also in the other seasons and stations where this variable was selected.

Table 3. Most frequently selected meteorological explanatory variables for each season. The (+) and (−) signs indicate whether PM_{10} concentrations have a positive or negative relationship with the explanatory variable. For wiggly terms (like, for example, Julian day), these signs only represent an average behavior. Variables in each season are sorted by decreasing frequency of occurrence.

Spring	Summer	Autumn	Winter	Year
wind gust (−)	Julian day (−)	wind gust (−)	wind gust (−)	daily precip (−)
CBL depth (−)	wind gust (−)	CBL depth (−)	CBL depth (−)	wind gust (−)
y. precip. (−)	a. temp. (+)	y. precip. (−)	temperature (−)	Julian day (−)
rel. humidity (−)		daily precip (−)	y. precip. (−)	y. precip. (−)
net irradiance (−)			net irradiance (+)	d. s. front (+)
daily precip. (−)			daily precip (−)	CBL depth (−)
				temperature

Sunday ambient PM_{10} concentrations are decrased by 12% compared to Monday on average over the 9 stations selected for the yearly data. Assuming that the primary aerosol emissions are similar during all the weekdays, the increase during weekdays might be attributed, on the one hand to the production of secondary aerosols and on the other to a possible buildup of aerosols in consecutive days with high emissions. A similar weekly PM_{10} pattern was found by Zidek et al. (2002) for the city of Vancouver.

The explanatory variables that were chosen for more than half (at least 7) of the models are summarized in Table 3. Figure 3 shows the PM_{10} factors of the most important explanatory variables. To provide results from a representative sample of stations, the stations were separated into five site types: "urban street", "urban background", "suburban", "rural lowland" (which includes the two "rural highway" stations) and "rural mountain" (see Table 1). For each variable in Table 3, its relationship with PM_{10} for one station from each site type is shown in Fig. 3. Each row of plots in this figure refers to the same variable and each column refers to the same site type. If the variable in question was selected at more than one station from the same type, the station where the variable was selected first is shown. If the variable appeared at two stations of the same type in the same order, the station where the variable caused the largest reduction of AIC is shown. In the plots in Fig. 3, the shaded areas indicate two standard errors above and below the best estimates. The values of the smooth PM_{10} functions before exponentiation had the property of summing up to zero. A "rug" was added to the horizontal axis to show the distribution of the values of each explanatory variable across its range.

Wind gust is the most important variable in all seasons except summer where it is the second most important. Wind gust depends on average wind speed and on turbulence kinetic energy. Wind speed was also included as an explanatory variable; however, it was usually not preferred in the variable selection process. This is probably because wind gust carries information about turbulence in the atmosphere. Thus, including wind gust not only accounts for transport of PM_{10} due to the mean wind but also for turbulent mixing. Note that it would not be possible to include both wind speed and wind gust in the GAMs because they are highly correlated and one of them would always be removed in step 4 of the algorithm (see Sect. 3). Hooyberghs et al. (2005) show a negative linear relationship between wind speed and PM_{10} concentrations. The relationship found here between wind gust and PM_{10} is approximately exponential (Fig. 3).

The second most important variable, chosen in spring, autumn and winter is CBL depth. CBL depth affects PM_{10} concentrations by limiting the volume of turbulent mixing of PM_{10}. Figure 3 shows that an increase in CBL depth results in a decrease of PM_{10} as expected. Non-linear relationships

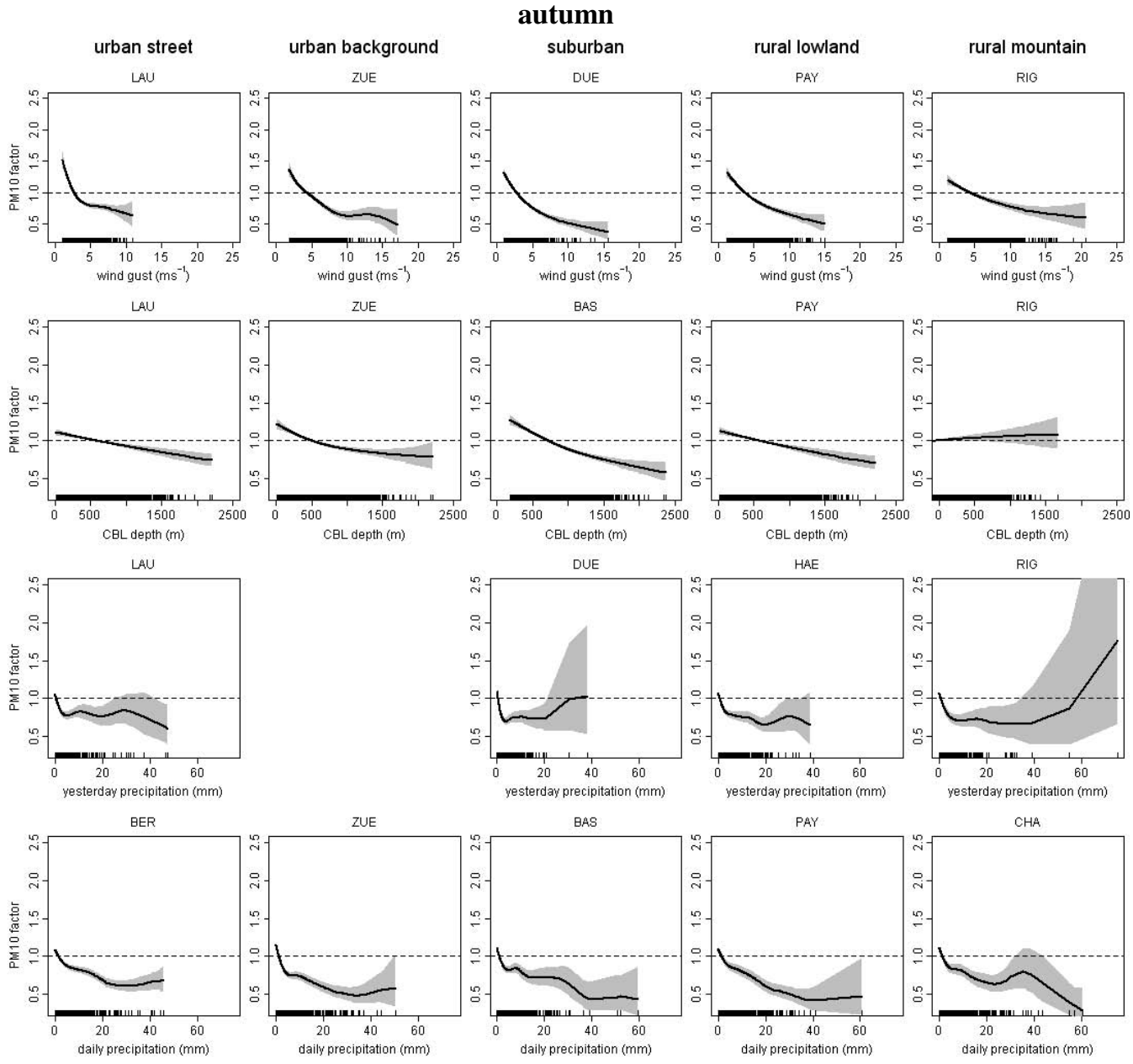

Fig. 3. Smooth functions of the most important explanatory variables for selected stations. Each row of plots corresponds to a different variable. Missing plots indicate that the variable in question was not selected in any stations of the corresponding category.

are encountered at many stations. This could be attributed to the fact that CBL depth was calculated of data from Payerne, a station in the Swiss plateau north of the Alps whereas the actual boundary layer characteristics of the stations included in this study are considerably affected by the presence of cities, mountains, valleys, lakes and other topographic particularities. Moreover, the important secondary aerosol production in Switzerland (Lanz et al., 2007, 2008) does not have a linear dependence on the aerosol precursors. Unlike all other stations, at the rural mountain station Rigi, the relationship between PM_{10} and CBL depth in autumn is positive. Given that Rigi is located above 1000 m, the levels of PM_{10} are affected by whether the station is in the boundary layer or above, rather than by the boundary layer depth per se.

Two other important variables that appear in spring, autumn and winter are daily precipitation and yesterday precipitation. Precipitation reduces considerably PM_{10} concentrations by wet deposition. In addition, if it is frontal precipitation, some polluted boundary layer air is replaced by clean air from aloft. As shown in Fig. 3, PM_{10} is particularly sensitive to low values of precipitation. PM_{10} levels reduce significantly for daily precipitation up to around 5 mm whereas for

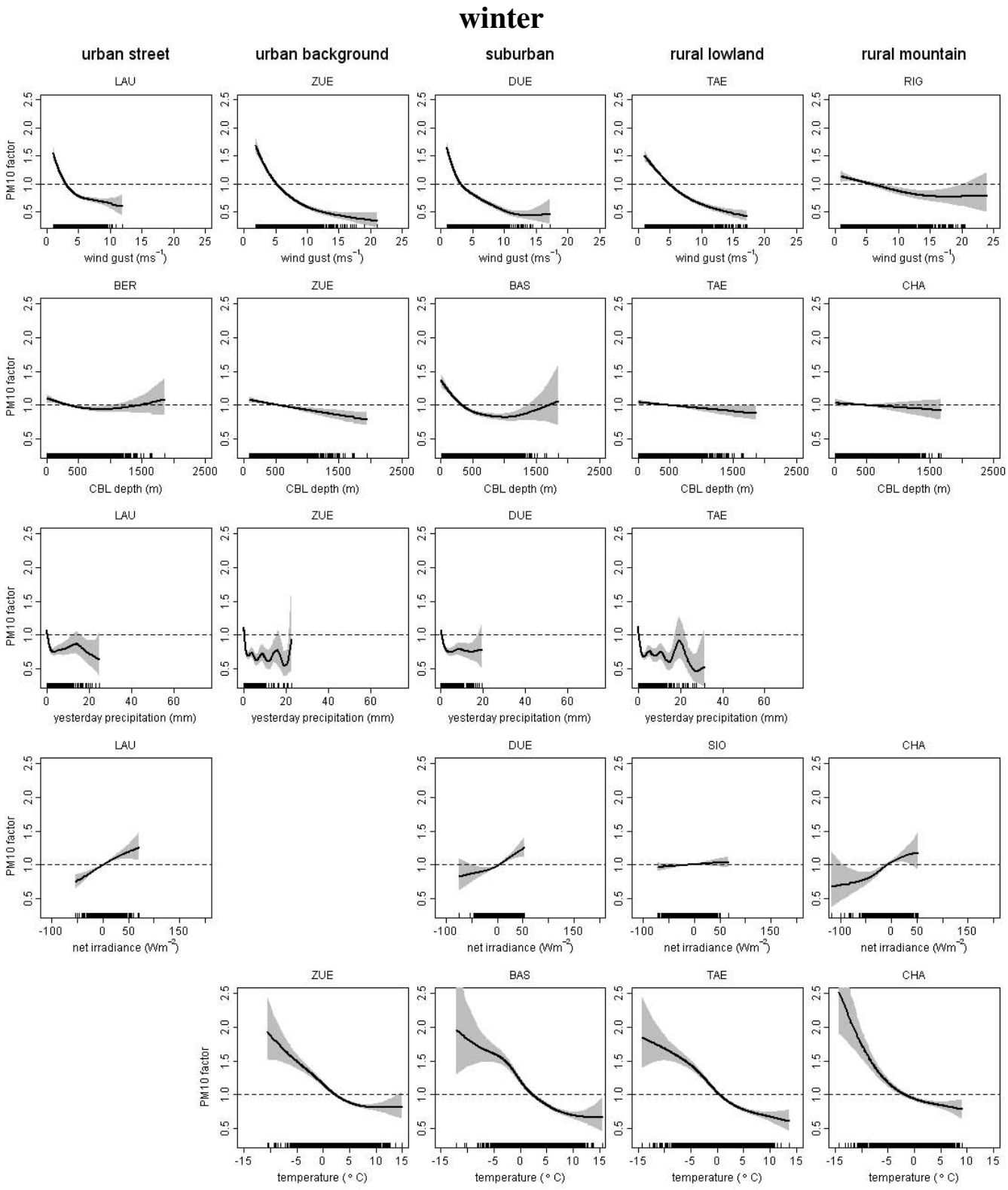

Fig. 3. Continued.

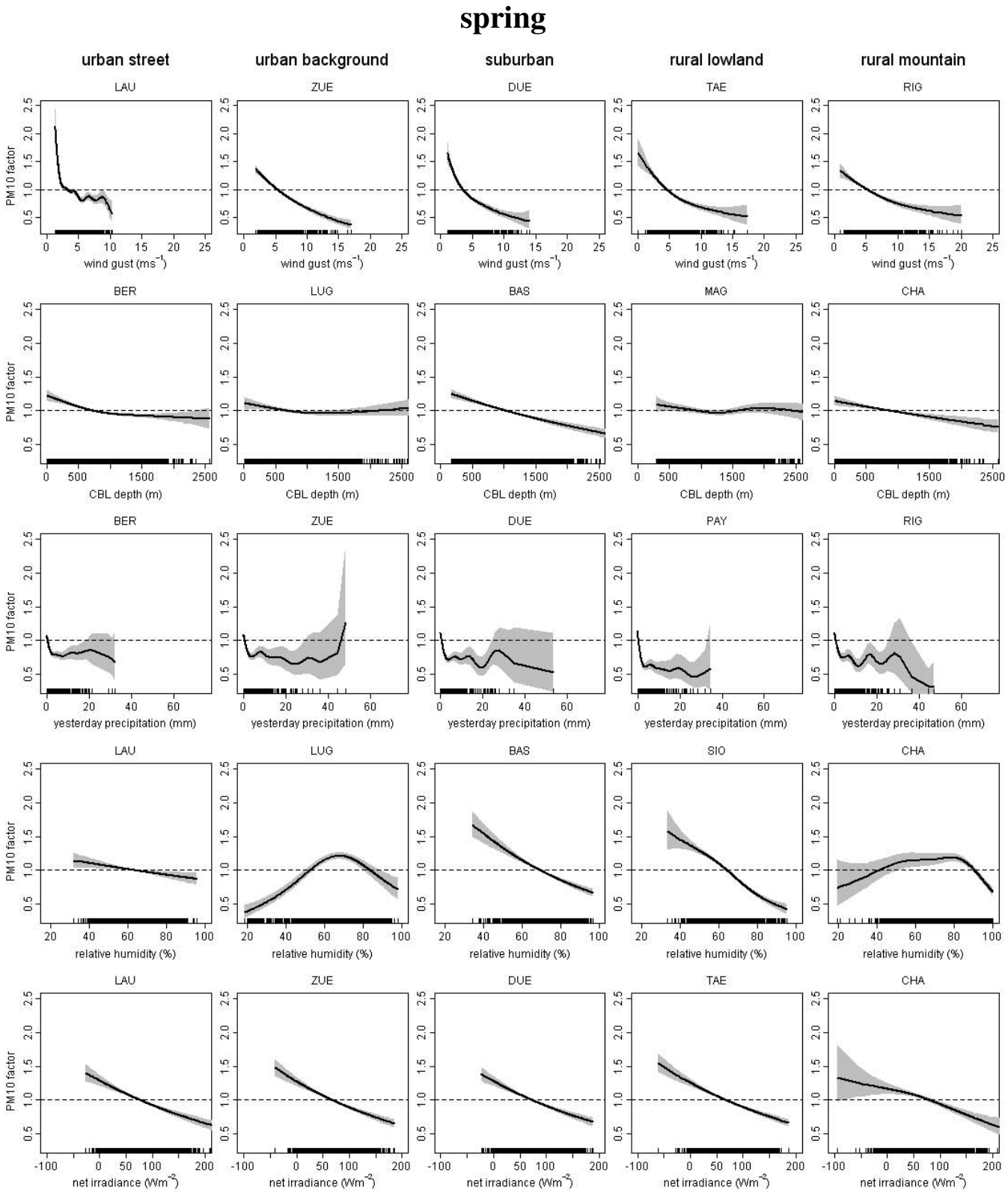

Fig. 3. Continued.

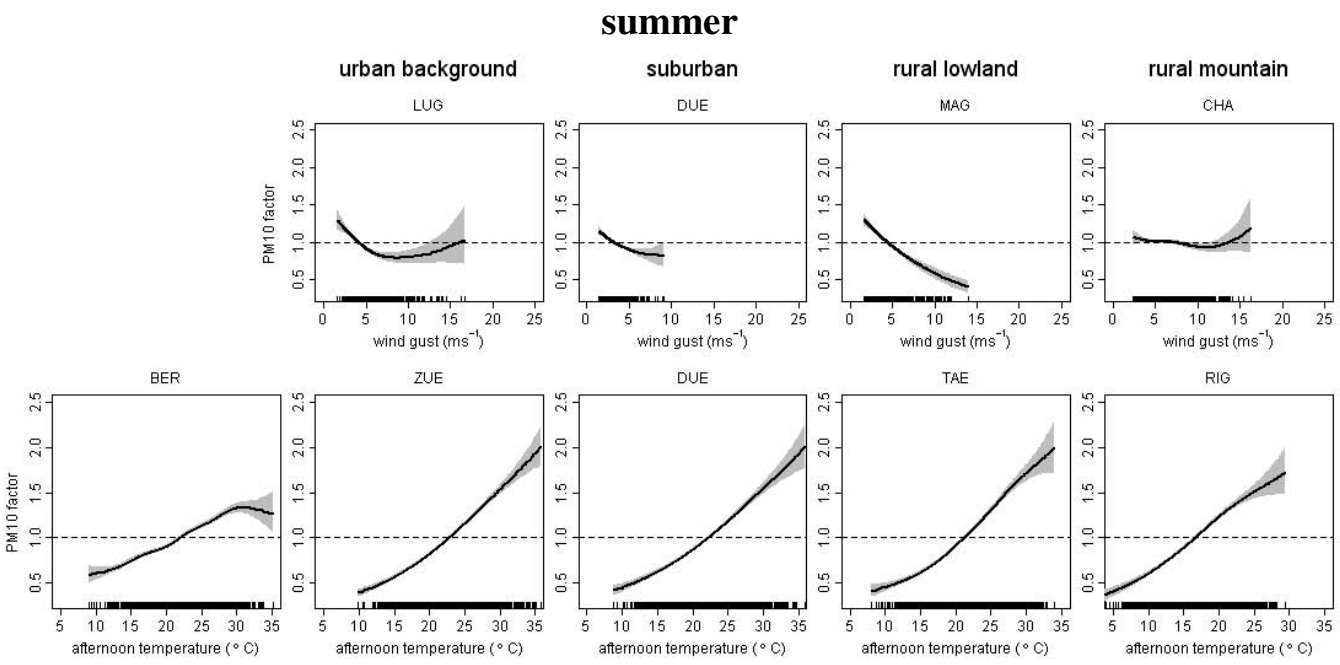

Fig. 3. Continued.

larger values of precipitation its effect diminishes. This feature would not be possible to depict by a linear relationship. For precipitation above 10 mm the effect on PM_{10} appears to be positive or strongly fluctuating at many stations. However, care should be taken when interpreting the results in regimes where data are sparse because the smooth functions have a large uncertainty in such regimes. Rugplots in Fig. 3 show that data are sparse above 10 mm of hourly precipitation and that the standard error becomes considerably large. The frequent selection of yesterday precipitation in the models indicates that, when investigating air pollution levels, it is not only important to take into account the current weather conditions but also the recent history of the weather. Current day precipitation and yesterday precipitation were not selected in summer where convective precipitation is encountered more frequently (Beniston et al., 1994). Convective precipitation typically lasts for a short time and exhibits a large spatial variability allowing for the presence of potentially high PM_{10} concentrations before the rain and some accumulation of new PM_{10} during the same day after the rain.

An important variable in spring and winter is net irradiance. Notably, this variable has opposite effects on PM_{10} during winter and spring. During spring, increasing values of net irradiance are associated with a strong decrease of PM_{10} concentrations. A possible explanation is that strong net irradiance contributes to large sensible heat flux which in turn drives the formation of deeper atmospheric boundary layers. However, in winter the relationship between PM_{10} concentrations and net irradiance is reversed with larger positive values of net irradiance contributing to an increase of PM_{10}. During winter, anticyclonic situations often create well-marked drainage flows from the Alps towards the Swiss Plateau. The cold air at the surface creates strong inversions, which in turn lead to radiation fog, high inversion fog (Hochnebel) and high levels of air pollution (Wanner and Hertig, 1984). While low negative values of net radiation occur with clear skies, the presence of Hochnebel introduces a positive term of long wave radiation in the net irradiance balance, which increases net irradiance. It is possible that through this mechanism, relatively high values of net irradiance lead to high concentrations of PM_{10}.

A further important explanatory variable for spring is relative humidity. Ambient aerosol mass concentrations of hygroscopic aerosol depend on relative humidity. On the one hand, such a dependency should not be detected by filter measurements. On the other hand, it is possible to see a dependency on relative humidity with beta attenuation monitors. For example, at low-temperature and high-relative humidity ambient conditions, air sucked into the measurement station warms-up to room temperature which in turn leads to a reduction of relative humidity and evaporation of water from hygroscopic aerosols. The relationship between PM_{10} and relative humidity is not the same for all stations (Fig. 3). Namely, there is a negative relationship for all sites except Lugano, Magadino (not shown) and Chaumont. These three sites exhibit a positive relationship for relative humidity below 60% and a negative relationship for relative humidity above 80% approximately. These relationships could be affected by the regional climate of these three sites. Southern Alps (where Lugano and Magadino are located) are known to be influenced by North Foehn episodes where clean air with low relative humidity descends from the Alps (Weber and Prévôt, 2002). North Foehn days amount to 9.7%, 7.6% and 4.2% of the days in March, April and May respectively.

Chaumont PM_{10} daily concentrations depend on whether the site is within the boundary layer or not. Polluted boundary layer air after ascending to elevated sites has increased relative humidity. In spite of the aforementioned information, the relationship between PM_{10} concentrations and relative humidity in spring remains unclear and requires further investigation.

Variable "afternoon temperature" was frequently selected in summer and a positive relationship between PM_{10} and afternoon temperature was identified at all stations (Fig. 3). Temperature has a particularly strong influence on PM_{10} in summer since a temperature increase from 10 to 35 °C increases PM_{10} by a factor of 4. This relationship can be the result of secondary aerosol production during warm summer days. The emissions of biogenic Volatile Organic Compounds (VOC), which amount to an estimated 24% of the total VOC emissions in Switzerland (Andreani-Aksoyoglu and Keller, 1995; Andreani-Aksoyoglu et al., 2008), depend on a number of meteorological variables which include temperature (Guenther, 1997). Besides, biogenic VOC include compounds with high yield, such as monoterpenes. Further explanations include good weather conditions (e.g. absence of frontal passages that could otherwise reduce PM_{10} concentrations) and enhanced resuspension of soil and road dust in warm days during summer (Vardoulakis and Kassomenos, 2008).

Temperature was selected 8 times in winter. Similarly to afternoon temperature in summer, temperature in winter has a marked effect on PM_{10} concentrations. Nevertheless, the relationship this time is inversed; low temperatures contribute to high PM_{10} concentrations by condensation of volatile compounds and possibly because of increased wood burning for space heating. Moreover, low temperature here can act as a proxy for stable boundary layer and low vertical mixing.

Most of the important variables selected for the whole year GAMs were also selected in the other seasons and their smooth functions are similar (not shown). The smooth function for temperature is an exception as the opposite response of PM_{10} to low and high temperatures is combined to give a negative relationship for low temperatures, positive relationship for high temperatures and a stationary point in between. Variable "days since front" that was only selected for whole year GAMs shows a decrease of PM_{10} for "days since front" less than 1 and an increase for "days since front" greater than 2. This indicates removal of PM_{10} by enhanced transport and wet deposition in the presence of a front and accumulation of PM_{10} after the frontal passage.

Julian day was selected often in summer implying that less PM_{10} variability is explained by meteorology during this season compared to winter. Factors that are not included in meteorology such as changes in anthropogenic emissions appear to have an important role in summer. The Julian day smooth functions provide a useful tool for the investigation of the meteorologically adjusted PM_{10} trends because they are able to detect non linear evolution of PM_{10} concentrations with time. The Julian day smooth functions are shown in Fig. 4. The stations shown for summer are selected in the same way as in Fig. 3 except that the stations are now split into six categories based on local emission characteristics. Namely, rural highway stations (Haerkingen and Sion) make a separate category. In the other seasons, all stations where Julian day was selected by the variable selection algorithm are shown.

All Julian day smooth functions shown in Fig. 4 have an overall decreasing trend which is interpreted to be at least to some extent the result of reduced PM_{10} emissions due to the implementation of emission reduction measures and technological improvements (e.g. vehicles with more efficient engines and catalytic converters). The change in mostly traffic and industrial precursor emissions (NO_x, SO_2, VOCs) of secondary aerosols is very likely responsible for the trend as well (Vestreng et al., 2007, 2008; Stemmler et al., 2005). The reduction of the PM_{10} factors is more pronounced in most of the 1990s whereas it is not as steep or even increases in the late 1990s and early 2000s. This evolution of PM_{10} is consistent to the GAINS model calculations of PM_{10} emissions and to the emissions of NO_x, non-methane volatile organic compounds, SO_2 and NH_3 as estimated by the European Monitoring and Evaluation Programme (Monks et al., 2009). It is not clear why at some stations PM_{10} concentrations increased in the early 2000s. In a source apportionment study which was carried out for London, UK similar trends were identified and the increase of PM_{10} in the aforementioned period was attributed to increased traffic emissions (Fuller and Green, 2006). In Switzerland, the share of diesel vehicles has been increasing in the last two decades and the increase in the period between 2000 and 2009 has been faster than the increase in the period between 1990 and 1999 (Fig. 5). This is particularly true for diesel passenger cars (Fig. 5) whose share was increasing by $0.099\%\ yr^{-1}$ on average in the 1990–1999 decade whereas in the 2000–2009 decade it is increasing by $1.4\%\ yr^{-1}$ as estimated by linear regression of diesel passenger car share versus year for the two decades respectively. A further local maximum appears in 1995 or 1996 at some stations in summer and spring.

To identify an overall trend in PM_{10} emissions, GAMs were created for yearly data and the corresponding Julian day smooth functions were estimated. This is shown in the last row of plots in Fig. 4. Strong seasonal features such as the 1995 maximum in the spring Lausanne PM_{10} factor are largely smoothed out in the yearly trend. Also in the yearly data there is an overall decrease of PM_{10} that is interrupted by two local maxima around 1996 and 2003. Two urban background stations, Zurich and Lugano (not shown) did not show a maximum in the 1990s. To better quantify and summarize the PM_{10} trends for all stations and seasons, an analysis of the PM_{10} trends by linear regression of the daily averages of PM_{10} values before and after meteorological adjustment is presented in Sect. 4.3.

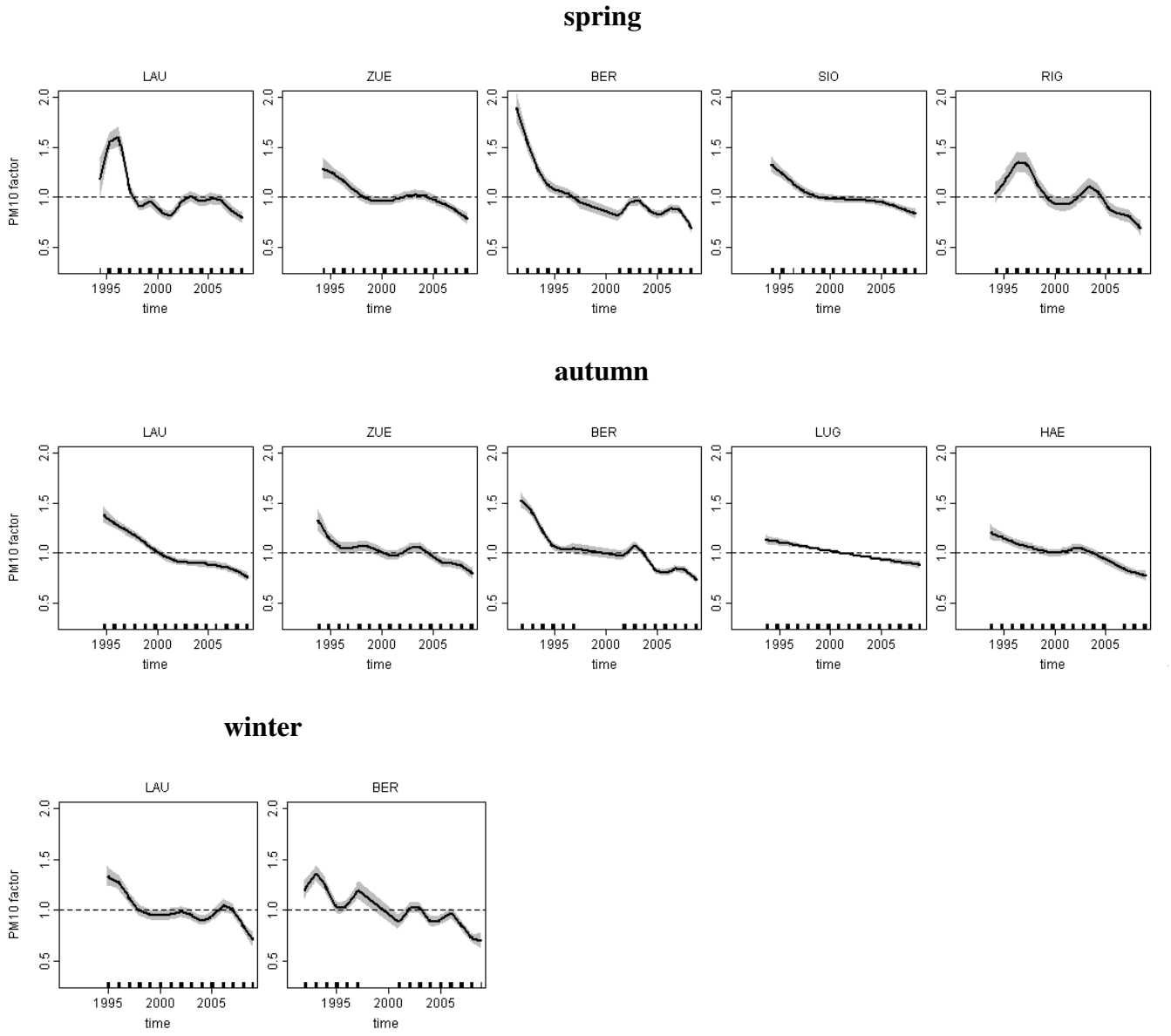

Fig. 4. Plots of the Julian day PM_{10} factor for selected stations. For summer, stations were selected by category. For all other seasons, all stations where this variable was selected are shown.

Considering the generality of the selected sets of explanatory variables and their relationship to PM_{10}, they are based on data from the NABEL measurement network and they are best applicable to the aforementioned sites. Nevertheless, they represent universal mechanisms of dispersion, dilution and formation of PM_{10} and are therefore expected to be suitable for other locations with similar climatic characteristics. However, testing is required before using statistical models at conditions different from those they were initially developed for. Considering the applicability of the proposed GAMs to other species, it is limited because deposition, resuspension and the response of various species to some meteorological variables such as temperature, solar irradiance and relative humidity depends strongly on the examined species.

4.2 Model performance

To evaluate the GAMs, the deviance explained (Wood, 2006) was used. Deviance explained quantifies which part of the observed variance is reproduced by the GAM. As shown in Table 4, winter was the season with the highest deviance explained reaching on average 65%. Summer had an almost equally high deviance explained of 64% and at the same

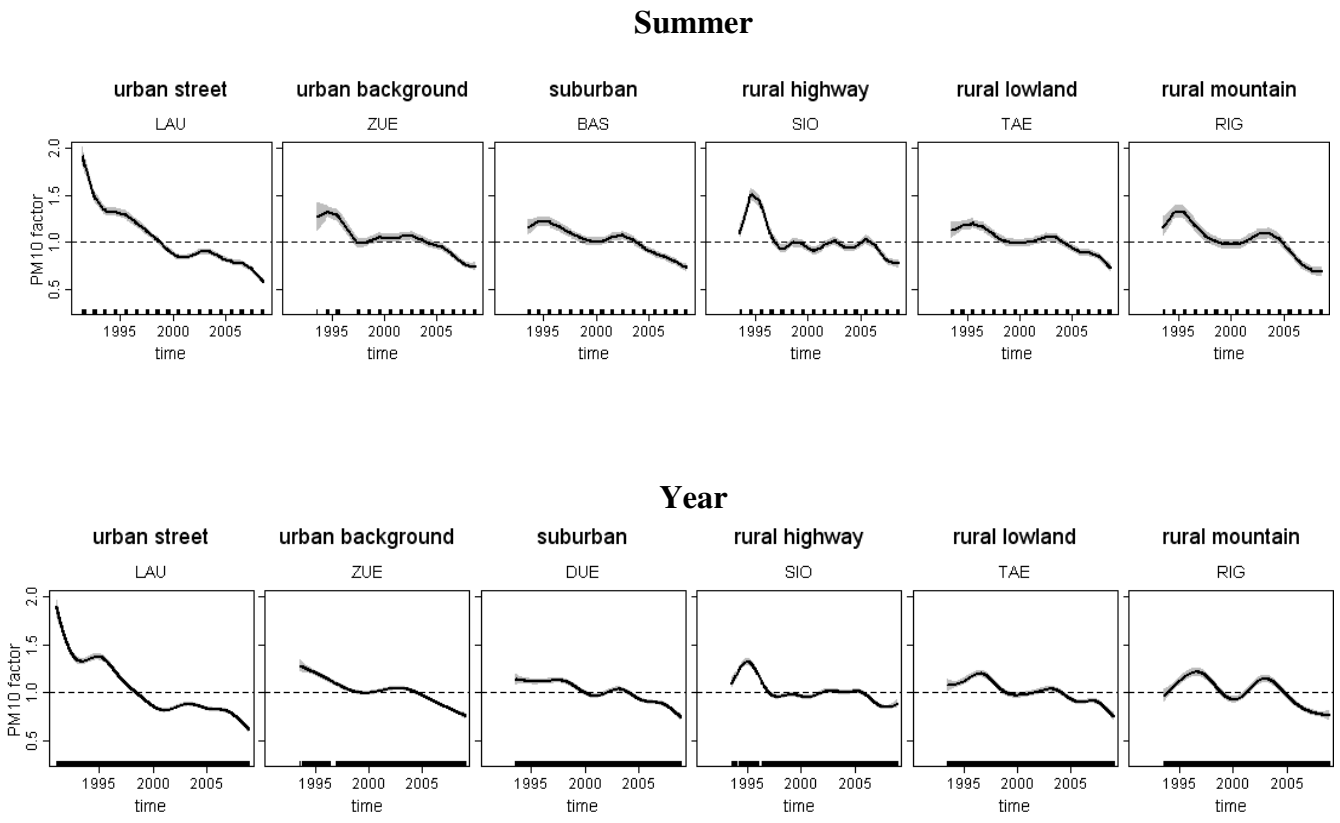

Fig. 4. Continued.

time a relatively small number of 6.4 selected explanatory variables. In spring an average of 8.2 selected covariates could explain on average only 56% of the observed variance, which indicates that the model has some difficulty in explaining the PM_{10} concentrations by means of the variables that are available for description of the meteorological variability. The yearly GAM runs yielded models with a high 65% deviance explained on average and a high number of selected explanatory variables (11.1). It should be noted that the deviance explained varied considerably from station to station. For example, in winter where the highest average deviance explained was encountered, the rural mountain stations of Chaumont and Rigi had rather low values of deviance explained (38% and 48% respectively) indicating that for the special weather conditions in mountainous areas the available meteorological variables are not capable of describing the effect of meteorology on PM_{10} concentrations. Moreover, due to the sites' elevation, PM_{10} concentrations are not only affected by local meteorology and emissions but by long-range transboundary transport as well.

Another way to assess model performance is to estimate the extent to which the year-to-year variability of meteorologically adjusted values is reduced. For this purpose, the mean squared error MSE (Wilks, 2006) was calculated according to the formula

$$\mathrm{MSE} = \frac{1}{m-2}\sum_{i=1}^{m} R_i^2 \tag{5}$$

where m is the number of data points used for the linear regression of the daily average PM_{10} concentrations versus time (see Sect. 4.3) and R_i are the model residuals defined as the difference of the predicted by the linear model minus the observed daily PM_{10}. MSE was calculated for the observed and adjusted PM_{10} values. The ratio of adjusted over measured MSE is tabulated in Table 4. The PM_{10} variability after meteorological adjustment in winter is only 27% of the observed variability. In spring, despite the relatively low deviance explained of the model estimates, the MSE ratio is 38% indicating a strong reduction of the variability of the PM_{10} values after meteorological adjustment. A smaller reduction of variability is observed in summer and autumn. The variability of the raw PM_{10} concentrations in those seasons is already rather low, as indicated by the respective MSE_{meas} values.

As already mentioned, 14–18 years of data were available for all stations. Although this is considered to be a sufficient amount of data to construct reliable GAMs, it is expected that such an analysis can be carried out with less data too. For example, data from 1994 until 2008 are available for Zurich station. A series of GAMs that were constructed using winter data since 1996, 1998, 2000, 2002 and 2004 showed that the

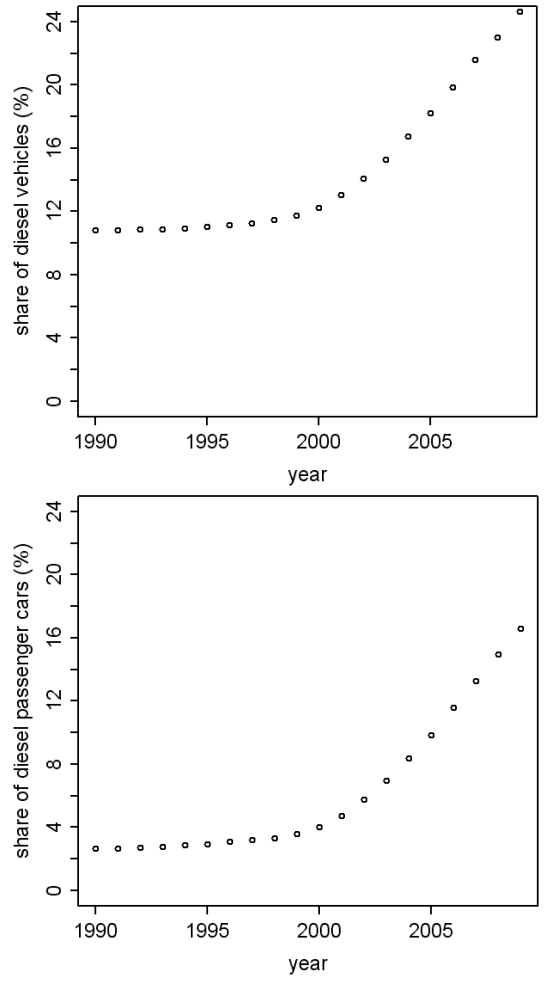

Fig. 5. Share of diesel vehicles in relation to the total of vehicles (top panel) and diesel passenger cars in relation to the total of passenger cars (bottom panel). Data from the Swiss Federal Statistical Office (2010).

Table 4. Seasonal averages of the deviance explained, number of covariates, measured MSE, adjusted MSE and the ratio of adjusted over measured MSE.

	dev. expl (%)	n. o. covariates	MSE_{meas} $(\mu g\,m^{-3})^2$	MSE_{adj} $(\mu g\,m^{-3})^2$	MSE ratio
Spring	56	8.2	22.14	10.43	0.38
Summer	64	6.4	8.88	4.43	0.41
Autumn	60	8.0	12.00	5.46	0.47
Winter	65	7.7	39.02	8.88	0.27
Year	65	11.1	8.4	4.7	0.52

resulting GAMs were quite consistent for the datasets starting in 2002 or for longer datasets i. e. for a minimum of seven years of data. Even fewer years of measurements are needed for analyzing full year datasets.

4.3 PM_{10} trends before and after meteorological adjustment

The trends of the PM_{10} concentrations in the period from 1991 to 2008 were estimated by linear regression of the daily average PM_{10} concentrations versus time. This was done for PM_{10} measurements and for the PM_{10} values that were adjusted for meteorology using relationship (4). The regression equations read

$$\text{daily average measured } PM_{10} = c_1 + c_2\,\text{Julian day} + \varepsilon \quad (6)$$

$$\text{daily average adjusted } PM_{10} = d_1 + d_2\,\text{Julian day} + \varepsilon \quad (7)$$

The estimated slopes c_2, d_2 of the regression lines were multiplied by 365 to represent yearly PM_{10} changes. The results of this process are summarized in Fig. 6 for all seasons and all stations. One should keep in mind that investigating the linear trends is a simplification because, as already discussed, the evolution of PM_{10} concentrations during the period in question is often non-linear, especially in winter. All slopes are shown with their 95% confidence intervals. In addition to the results for each station, the last value called "AVG" in each plot indicates the slope averaged over all stations. The confidence interval of the average was calculated by error propagation (e.g., Bevington and Robinson, 2003). This reads

$$\delta(PM_{10})_{avg} = \frac{1}{N}\sqrt{\sum_{i=1}^{N}\delta(PM_{10})_i^2} \quad (8)$$

where $\delta(PM_10)_{avg}$ is the average upper or lower confidence interval, $N = 13$ is the number of stations and $\delta(PM_{10})_i$ is the upper or lower confidence interval of the i-th station.

Figure 6 shows that PM_{10} trends are declining at almost all stations and seasons except the winter trend at the rural stations of Chaumont and Magadino. The confidence intervals of the measured and adjusted values largely overlap making the existence of a change in the PM_{10} trends due to the adjustment in many cases uncertain. However, it is discussed later that for some stations the meteorological adjustment had a considerable effect. In addition, the slopes of the adjusted trends have smaller uncertainty, which implies that the adjusted values can be used to identify significant trends from shorter time series.

Winter is the only season where the meteorological adjustment increased (in absolute terms) the slope of the PM_{10} trend line on average and at most stations. The largest changes were observed at the rural highway stations Haerkingen and Sion. Rural highway stations provide ideal locations for examining air pollution trends and the effect of weather because on the one hand the meteorological observations, not being affected by local urban features, are more accurate and representative and on the other hand strong local emissions of PM_{10} make it easier to detect appreciable changes in PM_{10} concentrations. Considerable reduction of the slope was also

observed in Magadino which is a rural station but its high annual average PM_{10} concentrations indicate that it is affected by relatively strong regional PM_{10} emissions and production. The stations with the largest yearly reduction of PM_{10} in winter (and in all other seasons) were the urban street stations of Bern and Lausanne. The fact that urban street and rural highway stations have the fastest decreasing PM_{10} concentrations indicates a reduction in traffic emissions of primary PM_{10}. Therefore, regulatory action and technology advances regarding vehicle emissions have had a considerable success in reducing PM_{10} concentrations.

The slopes of the PM_{10} trend lines after adjustment for meteorology are around zero at Lugano, Magadino and Rigi and positive at Chaumont. Since this behavior is only encountered in winter, it is reasonable to assume that the emission sector which caused this neutral trend is space heating. A particular space heating source to be considered is wood-burning since recent measurements (Szidat et al., 2007; Lanz et al., 2008, 2010; Sandradewi et al., 2008) demonstrate that wood-burning is a major source of particulate matter in winter both in the Swiss plateau and in the Alpine valleys. Unlike traffic emissions of PM_{10} and precursors, wood burning units have not reduced in the last two decades in Switzerland, their total number remaining almost stable at around 700 000 wood burning appliances (Primas et al., 2009). It should be noted that the PM_{10} trends in Lugano, Magadino, Rigi and Chaumont do not only depend on the meteorology and the emissions in Switzerland but they are considerably affected by neighboring countries too. Air pollution levels in the area of Ticino south of the Alps (including Lugano and Magadino) are considerably affected by the Milan area (Prévôt et al., 1997; Andreani-Aksoyoglu et al., 2004). Rigi and Chaumont are located at relatively high altitudes and are therefore affected by long-range transport. In addition, Chaumont is located close to the western border of Switzerland. Considering the predominant southwestern wind direction in the area (MeteoSwiss, 2010a), it is expected that PM_{10} levels at this station are rather affected by emissions in France than in Switzerland.

The finding that meteorological adjustment of PM_{10} trends in winter makes these trends more negative implies that the weather during winter in the 1990 and 2000 decades in Switzerland has changed in such a way that favors the accumulation of PM_{10}. A possible explanation for this feature is the evolution of the North Atlantic Oscillation (NAO) index, which has reduced considerably during the 1990 decade (Hurrell and Deser, 2010). High values of NAO index are linked to mild and wet winters whereas low values of NAO are linked to cold and dry winters which tend to increase levels of PM_{10}. NAO was one of the available explanatory variables which were not selected from the variable selection algorithm (see Table 2). This is attributed to the fact that the weather conditions associated with various NAO modes were described more directly by other explanatory variables.

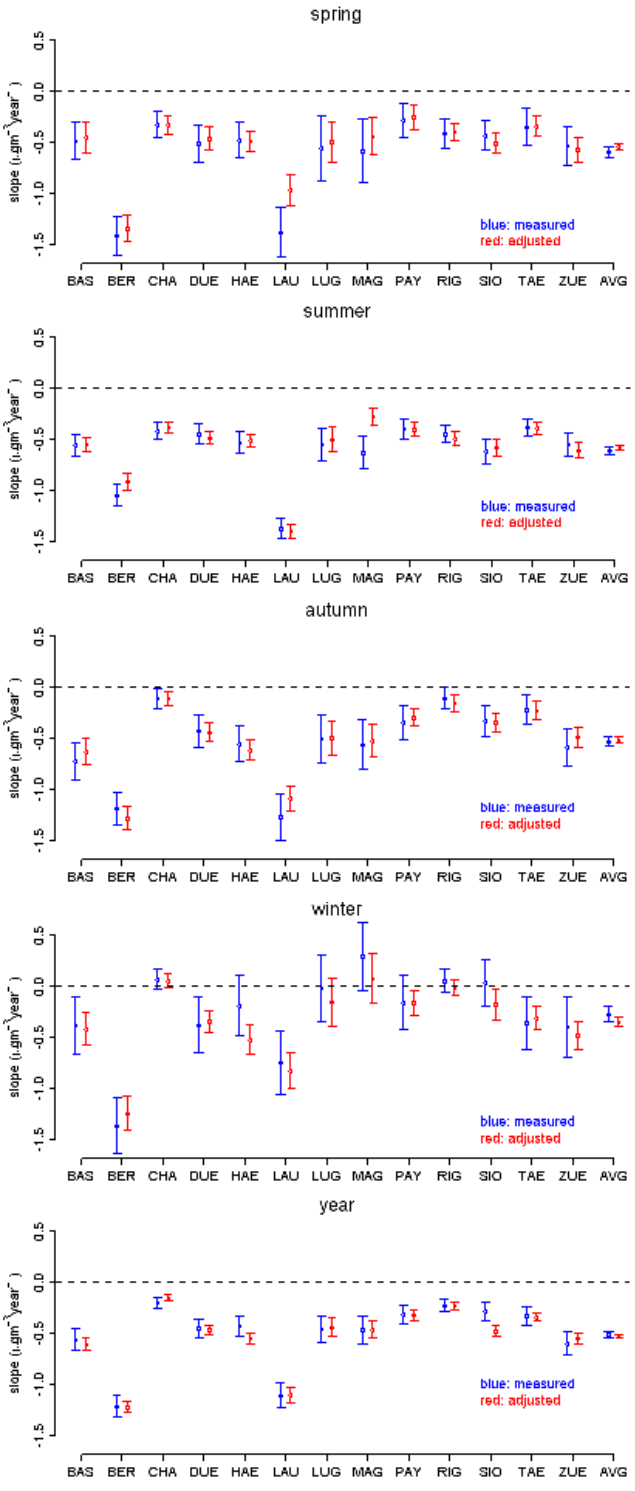

Fig. 6. Seasonal and yearly PM_{10} trends before and after the meteorological adjustment along with their 95% confidence intervals. "AVG" denotes the average over all stations.

The yearly trends shown in Fig. 6 have some similarities to the winter trends. The yearly trends before and after meteorological adjustment are tabulated in Table 5. On

Table 5. Trends of PM_{10} concentrations at all NABEL sites. The adjusted percentage trend is the result of dividing the adjusted trend by the 1991–2008 mean daily PM_{10} concentrations listed in Table 1.

Station	period of available data	raw trend ($\mu g\,m^{-3}\,yr^{-1}$)	met. adjusted trend ($\mu g\,m^{-3}\,yr^{-1}$)	met. adjusted percentage trend ($\%\,yr^{-1}$)	met. adjusted trend up to 1999 ($\mu g\,m^{-3}\,yr^{-1}$)	2000–2008 met. adjusted trend ($\mu g\,m^{-3}\,yr^{-1}$)
BAS	1993–2008	−0.56	−0.61	−2.4	−0.81	−0.85
BER	1991–2008	−1.2	−1.2	−3.1	−3.4	−1.1
CHA	1993–2008	−0.20	−0.15	−1.2	−0.37	−0.15
DUE	1993–2008	−0.45	−0.47	−1.8	−0.30	−0.49
HAE	1993–2008	−0.43	−0.55	−1.9	−1.0	−0.73
LAU	1994–2008	−1.1	−1.1	−3.3	−2.8	−0.4
LUG	1993–2008	−0.46	−0.44	−1.3	−0.71	−1.1
MAG	1993–2008	−0.47	−0.46	−1.5	−0.53	−0.49
PAY	1993–2008	−0.31	−0.32	−1.4	−0.24	−0.36
RIG	1993–2008	−0.23	−0.23	−1.7	−0.23	−0.36
SIO	1993–2008	−0.29	−0.48	−1.8	−1.5	−0.36
TAE	1993–2008	−0.33	−0.34	−1.6	−0.41	−0.37
ZUE	1993–2008	−0.60	−0.55	−2.0	−1.0	−0.67
AVG		−0.51	−0.53	−1.9	−1.0	−0.57

average, a small reduction of the PM_{10} trend after adjustment for meteorology is observed. The stations which actually have a considerable reduction of their PM_{10} trends after adjustment for meteorology are the rural highway stations of Haerkingen and Sion where the adjusted trends are lower by 0.12 and 0.19 $\mu g\,m^{-3}\,yr^{-1}$ respectively (Table 5). This probably reflects the aforementioned winter behavior of the PM_{10} trends in those stations because in the other seasons the meteorological adjustment, although narrowed considerably the confidence intervals, only caused little change in the best estimates of the slope. Velders and Matthijsen (2009) reported yearly trends of $-0.97\,\mu g\,m^{-3}\,yr^{-1}$, $-0.74\,\mu g\,m^{-3}\,yr^{-1}$ and $-0.79\,\mu g\,m^{-3}\,yr^{-1}$ for rural, urban background and urban street stations respectively, in the Netherlands from 1992 to 2007. Although these trends have similar magnitudes to the ones reported here, there are some notable differences. Namely, in the current study, rural stations have smaller trends than urban stations and urban background stations have smaller trends than urban street stations. The respective averages for rural, urban background and urban street stations are −0.37, −0.53 and $-1.2\,\mu g\,m^{-3}\,yr^{-1}$ (Table 5). Stedman (2002) reported decreasing PM_{10} trends for 8 city centre stations in the UK, these trends ranging between $-0.9\,\mu g\,m^{-3}\,yr^{-1}$ and $-1.9\,\mu g\,m^{-3}\,yr^{-1}$ for data between 1992 or 1993 until 2000. These trends are also comparable (although somewhat larger) to the trends found in Swiss cities. In a further related study, Spindler et al. (2004) report a negative trend of roughly $-1.5\,\mu g\,m^{-3}\,yr^{-1}$ based on measurements at some stations in the area of west Saxony, Germany, although an exponential instead of a linear relationship was actually chosen to describe the decline of PM_{10} in that area.

No literature discussing PM_{10} trends on the basis of seasonal data is known to the authors. The average values of the adjusted trend per season found in this study are $-0.54\,\mu g\ m^{-3}\ yr^{-1}$, $-0.58\,\mu g\ m^{-3}\,yr^{-1}$, $-0.52\,\mu g\ m^{-3}\,yr^{-1}$, $-0.35\,\mu g\ m^{-3}\,yr^{-1}$ and $-0.53\,\mu g\ m^{-3}\,yr^{-1}$ for spring, summer, autumn, winter and yearly data respectively.

In autumn the adjusted trend at the urban street station Lausanne is less decreasing. A similar effect of reduced slope after meteorological adjustment is also evident in the stations of Bern and Magadino in summer and Lausanne in spring. Lausanne and the other urban street station, Bern have the steepest trends among all stations in all seasons implying considerable PM_{10} reductions from the traffic sector.

The importance of the aforementioned long-term PM_{10} changes at each site depends on the average level of PM_{10} concentrations at the site in question. In order to put the PM_{10} trends in this context, the adjusted trends were calculated as the percentage of the mean PM_{10} observations during the period in question (see Table 1). The results are tabulated in Table 5. The urban street stations at Bern and Lausanne apart from having the largest trends, they also have the largest percentage trends amounting to 3.1 and 3.3% yr^{-1} respectively. The average percentage trend over all stations is $-1.9\%\,yr^{-1}$ with a range of −1.2 to $-3.3\%\,yr^{-1}$.

As already noted, visual inspection of Fig. 4 reveals that the adjusted PM_{10} trends do not have a uniform behavior throughout the period between 1991 and 2008. A further examination of the adjusted PM_{10} trends was carried out by separating the PM_{10} GAM estimates before 2000 and from 2000 onwards and estimating the line fitted by linear regression of PM_{10} concentrations versus time in each period. At most stations the trends before and after 2000 differ by less

than $0.4\,\mu g\,m^{-3}\,yr^{-1}$, in absolute terms (Table 5). Bern and Lausanne however exhibit considerably larger differences; The PM_{10} trend at Bern increased from $-3.4\,\mu g\,m^{-3}\,yr^{-1}$ in 1991–1999 to $-1.1\,\mu g\,m^{-3}\,yr^{-1}$ in 2000–2008. The slope at Lausanne similarly increased from $-2.8\,\mu g\,m^{-3}\,yr^{-1}$ in 1994–1999 to $-0.4\,\mu g\,m^{-3}\,yr^{-1}$ in 2000–2008.

In addition to the slopes of the linear regressions, it is useful to see the effect of the meteorological adjustment on the actual PM_{10} concentrations. Figure 7 shows the yearly averaged PM_{10} concentrations before and after the adjustment for meteorology and their trend lines. One station from each one of the six categories mentioned in Sect. 4.1 is included. The stations with the largest changes in their PM_{10} trend after meteorological adjustment were preferred.

Winter has the highest PM_{10} variability and the highest reduction of PM_{10} variability after the meteorological adjustment (see MSE values in Table 4). For example, as shown in Fig. 7, extreme high PM_{10} concentrations in winter seasons 1992, 1997, 2003 and 2006 in Bern were heavily reduced after meteorological adjustment. Similar effects are seen in other seasons too (e.g. spring 1996 in Lausanne station). Examination of all plots in Fig. 7 (and the remaining plots which are not included in this figure) shows that GAMs have a good skill in removing PM_{10} variability even in cases where PM_{10} concentrations were unusually high because of weather conditions.

4.4 Model validation

The models described above were developed using a random 90% of the available observations. The remaining 10% of the observations were used to validate the models obtained from the 90% of the observations. In this process, the values of the explanatory variables which were chosen in the GAMs were substituted into the GAM formulas to give predictions of PM_{10} values. These predictions were then compared to the corresponding PM_{10} measurements.

A graphic comparison between model predictions and observations is done by examination of scatter plots (Fig. 8). A one-to-one line was added to facilitate comparison to the ideal model. The factor-of-two scatter is indicated by dashed lines. Some points are missing from these plots either because of missing PM_{10} measurements or missing meteorological observations in the selected 10% of the days. The stations included in Fig. 8 are the same as in Fig. 7.

To validate quantitavely the GAMs, the fraction of daily GAM predictions which lie between 50% and 200% of the corresponding measurements was calculated. This is the so-called "factor of 2" (FAC2) statistic (Chang and Hanna, 2004) and reads:

$$\text{FAC2} = \text{fraction of data that satisfy } 0.5 \leq \frac{PM_{10\,\text{predicted}}}{PM_{10\,\text{observed}}} \leq 2.0 \quad (9)$$

It follows that for an ideal model, FAC2 = 1. Data points which lie in the area within the dashed lines in the scatterplots in Fig. 8 satisfy Eq. (9).

Visual inspection of the scatterplots in Fig. 8 reveals a very good predictive skill of the GAMs since the vast majority of the data fall within the factor of two area marked by the dash lines. However, in most stations in summer, autumn and spring, some underprediction of PM_{10} values is observed for high (above 30–40 $\mu g\,m^{-3}$) PM_{10} measurements. Such deviation can occur in cases where irregular emissions such as, for example, agricultural burning or fireworks impact the measurement site.

The FAC2 values are very high, often approaching unity. Their averages over all stations are 0.90, 0.98, 0.92, 0.93 and 0.93 for spring, summer, autumn, winter and yearly data respectively. The FAC2 values for some individual stations are included in Fig. 8. FAC2 values at the mountainous sites at Rigi and Chaumont, although still satisfactory, are somewhat lower (usually between 80%–90%).

The linear dependence of the predicted versus the measured PM_{10} concentration was estimated using the Pearson correlation coefficient. A relatively high linear dependence was found with the average correlation coefficient values over all stations being 0.62, 0.78, 0.72, 0.72 and 0.72 for spring, summer, autumn, winter and yearly data respectively.

5 Conclusions

The trends of PM_{10} and the effect of meteorology were investigated for 13 air quality stations in Switzerland for the period between 1991 and 2008. This was done by constructing Generalised Additive Models (GAMs) which incorporate non-parametric relationships between PM_{10} and meteorological and time variables. These relationships were based on quality-checked meteorological and PM_{10} long-term observations including a wide spectrum of meteorological variables with good spatial and temporal coverage.

Most of the estimated functions provided fairly intuitive answers with regards to which direction PM_{10} concentrations change when a change of a certain meteorological variable occurs. For example, it was found that PM_{10} concentrations have negative relationships with wind gust, yesterday precipitation and convective boundary layer depth whereas they have positive relationships with afternoon sunshine duration and afternoon temperature. The contribution of this study was to provide further insight in those relationships by quantifying them and accounting for non-linearities. For instance, a small precipitation rate strongly reduces PM_{10} concentrations whereas a further increase in the precipitation rate has no further considerable effect. Another interesting finding is the importance of each meteorological variable in the different seasons. Apart from wind gust which was one of the most important variables in all seasons, large interseasonal differences were found with regards to the preferred variables.

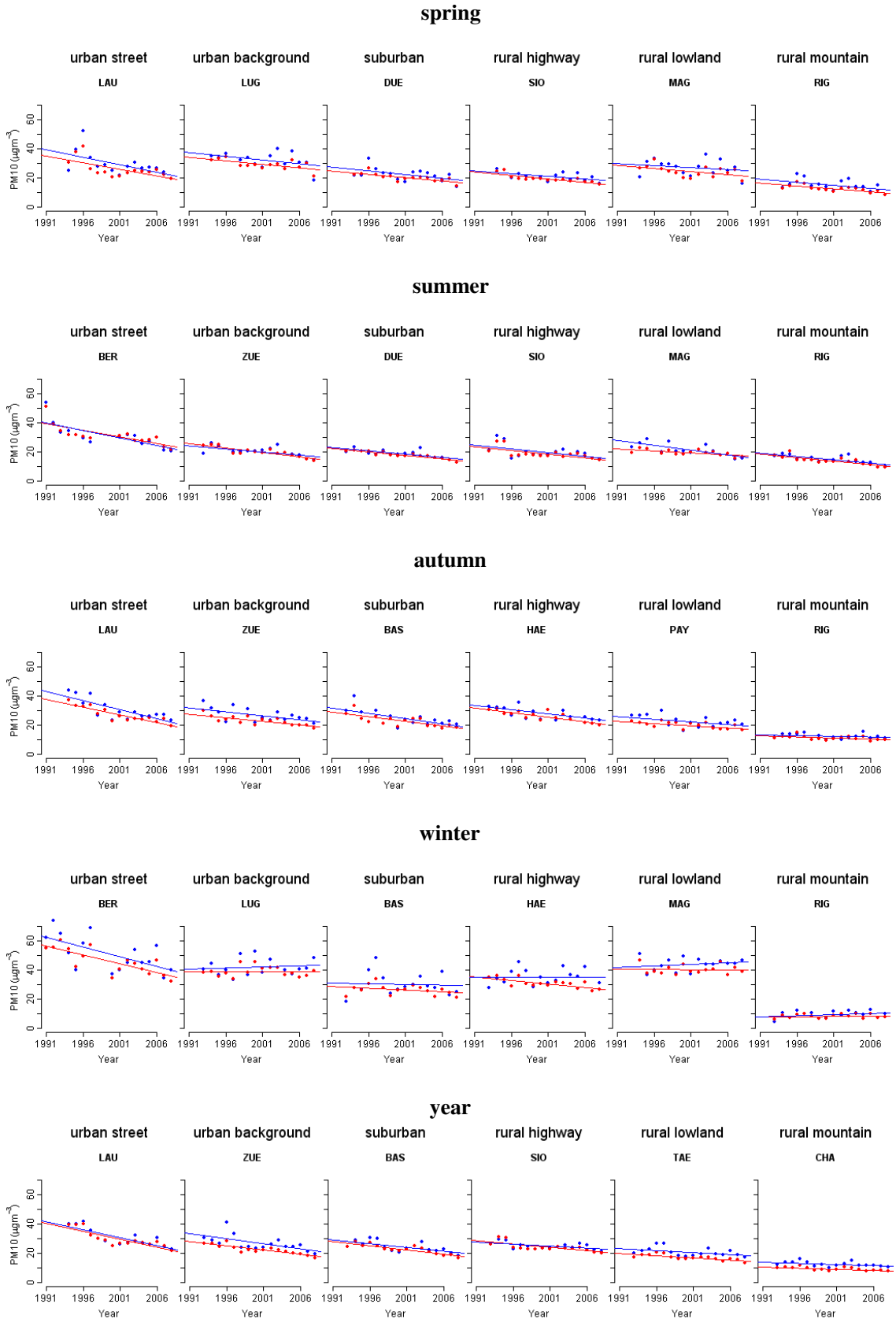

Fig. 7. Raw (blue) and adjusted for meteorology (red) seasonal average PM_{10} values. The respective trend lines obtained by linear regression are also plotted.

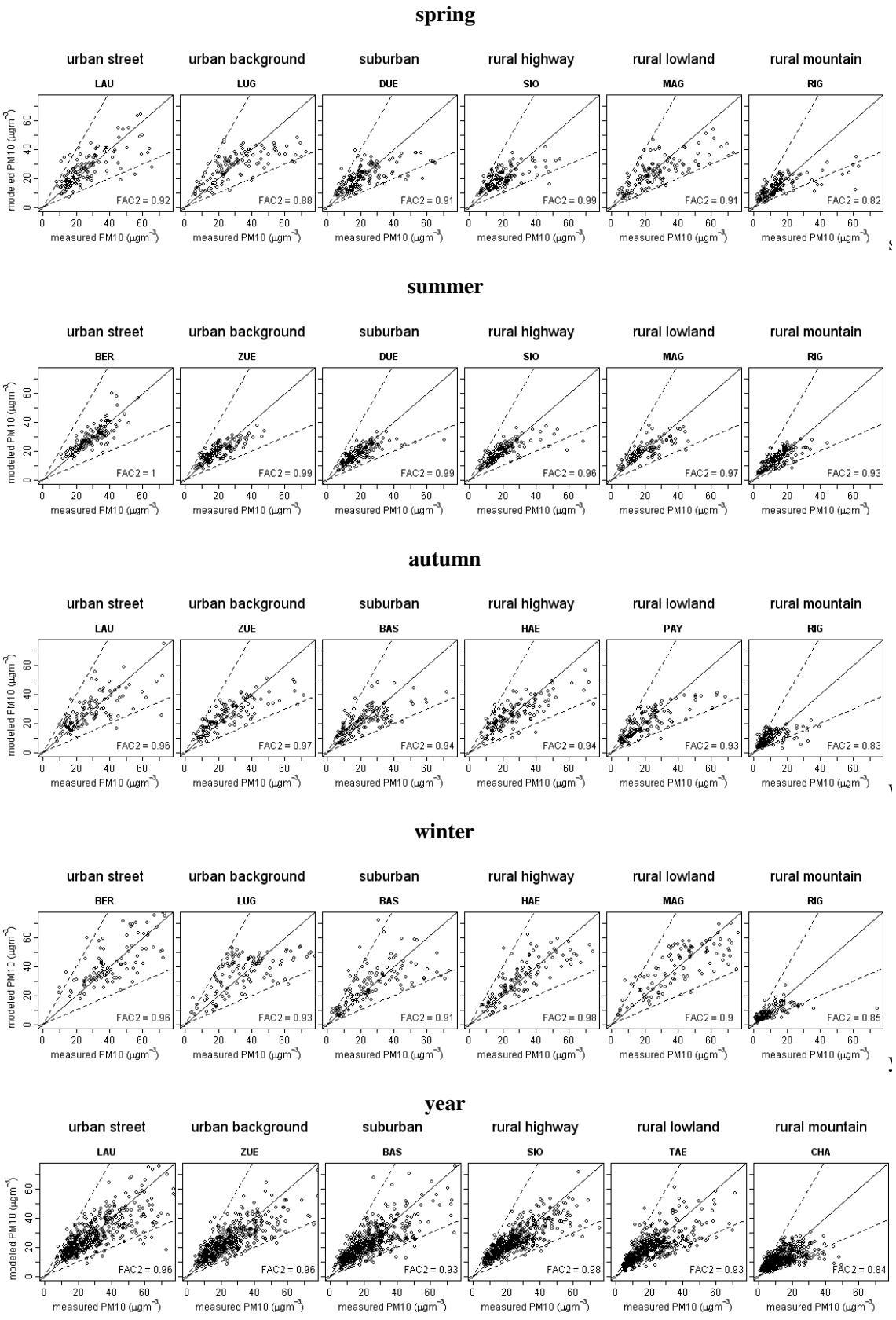

Fig. 8. Scatter plots of measured versus predicted PM_{10} concentrations using a random 10% of the data. Dashed lines indicate the factor of two area.

The convective boundary layer depth was important in winter, spring and autumn while PM_{10} concentrations appear to be not so sensitive to changes in the boundary layer depth during summer where deep convective boundary layers form relatively often. The rate of precipitation on the current and the previous day was frequently selected for winter, autumn and spring and not so frequently selected for summer where convective precipitation is more frequent.

The variability of PM_{10} unrelated to meteorology (represented by the Julian day variable) was found to be important in summer and not so important in spring, winter and autumn. Examination of the Julian day smooth functions showed a non-linear trend in PM_{10} concentrations. A relatively fast yearly reduction of PM_{10} was observed for the years until 2000 and a slow reduction from 2000 on, especially at the urban street stations Bern and Lausanne.

The GAMs showed a good ability to reduce the observed PM_{10} variability in winter. The reduction of the PM_{10} variability after the adjustment for meteorology was lower in the other seasons, which anyway had a rather low variability of the raw PM_{10} values.

The strong effect of meteorology in PM_{10} concentrations was also reflected on the PM_{10} trends in winter. Removal of the effect of meteorology resulted in a more negative trend at most stations. In almost all seasons and stations, there was a downward trend of the adjusted PM_{10} concentrations during the period in question. The seasonal trends averaged over all stations amount to $-0.54\,\mu g\,m^{-3}\,yr^{-1}$, $-0.58\,\mu g\,m^{-3}\,yr^{-1}$, $-0.52\,\mu g\,m^{-3}\,yr^{-1}$, $-0.35\,\mu g\,m^{-3}\,yr^{-1}$ and $-0.53\,\mu g\,m^{-3}\,yr^{-1}$ for spring, summer, autumn, winter and yearly data, respectively. These trends correspond to respective percentage changes of $-2.0\%\,yr^{-1}$, $-2.2\%\,yr^{-1}$, $-1.8\%\,yr^{-1}$, $-1.1\%\,yr^{-1}$ and $-1.9\%\,yr^{-1}$.

The reduction of PM_{10} after adjustment for meteorology demonstrates that air pollution abatement policies in Switzerland have been effective to a certain extent. This also applies to EU countries surrounding Switzerland which affect air pollution levels in Swizterland through transboundary pollution. Air pollution abatement measures in Switzerland include the adoption of cleaner road vehicle technologies (Euro 1, 2, 3, and 4 emission standards), promotion of public transport and improvements in the rail and road infrastructure (Berger et al., 2009). The continuation of regulatory action towards the reduction of air pollution is expected to contribute to a further decrease of PM_{10} in the future. For instance, as of 2011 only Euro 5 vehicles will be imported in Switzerland (Swiss Federal Council, 2010b). An important feature of the Euro 5 technology is that passenger cars and light duty vehicles using diesel have to be equipped with particle traps. As a large fraction of particulate matter is due to secondary aerosols from precursor gases like NO_x, SO_2 and NH_3, future trends will depend a lot on the future emissions on these precursors. Especially for NO_x there is still a large reduction potential. Further recent measures include stricter regulation for emissions from construction equipment and stricter regulation for wood burning emissions (Swiss Federal Council, 2010a). The road infrastructure is planned to develop further so that traffic jams are reduced (Swiss Federal Council, 2010c). Some relief of the road network is also expected by the planned increase of the capacity and speed of rail transport (Swiss Federal Council, 2010c). Nevertheless, the actual PM_{10} trends in the future will also be affected by the increasing demand for transport and other particle and precursor emitting activities (Swiss Federal Council, 2010c).

The prognostic skill of the model was examined by model validation. The FAC2 statistic for different seasons ranged between 0.90 and 0.93 whereas the Pearson correlation coefficient ranged between 0.62 and 0.78 on average over all stations. Therefore, GAMs have considerable potential as a cheap tool for air quality forecasting, provided that a good weather forecast is available.

Acknowledgements. This study was supported by the COST fund of the Swiss State Secretariat for Education and Research. Many thanks to Urs Baltensperger and Ernest Weingartner for useful discussions. A considerable part of the data used in this study were provided by MeteoSwiss and the Swiss Federal Office for the Environment (FOEN). The NAO data have been supplied by Phil Jones. Data up to 1999 were downloaded from http://www.cru.uea.ac.uk/cru/data/nao/ and data after 1999 were downloaded from Tim Osborne's NAO webpage http://www.cru.uea.ac.uk/~timo/datapages/naoi.htm.

Edited by: W. Birmili

References

Andreani-Aksoyoglu, S. and Keller, J.: Estimates of monoterpene and isoprene emission from the forests in Switzerland, J. Atmos. Chem., 20, 71–87, 1995.

Andreani-Aksoyoglu, S., Prévôt, A. S. H., Baltensperger, U., Keller, J., and Dommen, J.: Modelling of formation and distribution of secondary aerosols in the Milan area (Italy), J. Geophys. Res., 109, D05306, doi:10.1029/2003JD004231, 2004.

Andreani-Aksoyoglu, S., Keller, J., Prévôt, A. S. H., Baltensperger, U., and Flemming, J.: Secondary aerosols in Switzerland and northern Italy: Modelling and sensitivity studies for summer 2003, J. Geophys. Res., 113, D06303, doi:10.1029/2007JD009053, 2008.

Akaike, H.: A new look at the statistical model identification, IEEE T. Automat. Contr., AC-19, 716–723, 1974.

Bayer-Oglesby, L., Grize, L., Gassner, M., Takken-Sahli, K., Sennhauser, F. H., Neu, U., Schindler, C., and Braun-Fahrländer, C.: Decline of ambient air pollution levels and improved respiratory health in swiss children, Environ. Health Persp., 113, 1632–1637, 2005.

Beniston, M., Rebetez, M., Giorgi, F., and Marinucci, M. R.: An analysis of regional climate in Switzerland, Theor. Appl. Climatol., 49, 135–159, 1994.

Berger, H.-U., Gueller, P., Mauch, S., and Oetterli, J.: Verkehrspolitische Entwicklungspfade in der Schweiz: Die letzten 50 Jahre, Rüegger Verlag, Zürich, ISBN 978-3-7253-0912-2, 2009.

Bevington, P. R. and Robinson, D. K.: Data reduction and error analysis for the physical sciences, McGraw Hill, New York, USA, 39–41, 2003.

Chang, J. C. and Hanna, S. R.: Air quality model performance evaluation, Meteorol. Atmos. Phys., 87, 167–196, 2004.

Creilson, J. K., Fishman, J., and Wozniak, A. E.: Intercontinental transport of tropospheric ozone: a study of its seasonal variability across the North Atlantic utilizing tropospheric ozone residuals and its relationship to the North Atlantic Oscillation, Atmos. Chem. Phys., 3, 2053–2066, doi:10.5194/acp-3-2053-2003, 2003.

Darlington, T. L., Kahlbaum, D. F., Heuss J. M., and Wolf, G. T.: Analysis of PM_{10} trends in the United States from 1988 through 1995, JAPCA J. Air Waste MA., 47, 1070–1078, 1997.

Easter, R. C. and Peters, L. K.: Binary homogeneous nucleation: Temperature and relative humidity fluctuations, nonlinearity, and aspects of new particle production in the atmosphere, J. Appl. Meteorol., 33, 775–784, 1994.

Eckhardt, S., Stohl, A., Beirle, S., Spichtinger, N., James, P., Forster, C., Junker, C., Wagner, T., Platt, U., and Jennings, S. G.: The North Atlantic Oscillation controls air pollution transport to the Arctic, Atmos. Chem. Phys., 3, 1769–1778, doi:10.5194/acp-3-1769-2003, 2003.

Empa: Technischer Bericht zum Nationalen Beobachtungsnetz für Luftfremdstoffe (NABEL), 2010.

European Parliament and the Council: Directive 2008/50/EC of the European Parliament and of the Council of 21 May 2008 on ambient air quality and cleaner air for Europe, Official Journal of the European Union, L 152, 1–144, 2008.

Freund, R. J. and Wilson, W. J.: Regression Analysis: Statistical modeling of a response variable, Academic Press, San Diego and London, 192 pp., 1998.

Fuller, G. W. and Green, D.: Evidence for increasing concentrations of primary PM_{10} in London, Atmos Environ., 40, 6134–6145, 2006.

Gehrig, R., Hueglin, C., Schwarzenbach, B., Seitz, T., and Buchmann B.: A new method to link PM_{10} concentrations from automatic monitors to the manual gravimetric reference method according to EN12341, Atmos Environ., 39, 2213–2223, 2005.

Gomiscek, B., Frank, A., Puxbaum, H., Stopper, S., Preining O., and Hauck H.: Case study analysis of PM burden at an urban and a rural site during the AUPHEP project. Atmos. Environ., 24, 3935–3948, 2004.

Guenther, A.: Seasonal and spatial variations in natural volatile organic compound emissions, Ecol. Appl., 7, 34–45, 1997.

Hastie, T. J. and Tibshirani, R. J.: Generalized Additive Models Chapman. & Hall/CRC., Boca Raton, 139–139, 1990.

Hooyberghs, J., Mensink, C., Dumont, G., Fierens, F., and Brasseur, O.: A neural network forecast for daily average PM_{10} concentrations in Belgium, Atmos. Environ., 39, 3279–3289, 2005.

Hueglin, C., Gehrig, R., Baltensperger, U., Gysel, M., Monn, C., and Vonmont, H.: Chemical characterization of $PM_{2.5}$, PM_{10} and coarse particles at urban, near-city and rural sites in Switzerland, Atmos. Environ., 39, 637–651, 2005.

Hurell, J. W. and Deser, C.: North Atlantic Climate Variability: The role of the North Atlantic Oscillation, J. Marine Syst., 79, 231–244, 2010.

Jackson, L. S., Carslaw, N., Carslaw, D. C., and Emmerson, K. M.: Modelling trends in OH radical concentrations using generalized additive models, Atmos. Chem. Phys., 9, 2021–2033, doi:10.5194/acp-9-2021-2009, 2009.

Jones, P. D., Jonsson T., and Wheeler, D.:Extension to the North Atlantic Oscillation using early instrumental pressure observations from Gibraltar and South-West Iceland, Int. J. Climatol. 17, 1433–1450, 1997.

Keller, J., Prévôt, A. S. H., Béguin, A. F., Jutzi, V., and Ordóñez, C.: Trends of Ozone and O_x in Switzerland from 1992 to 2007: Observations at selected stations of the NABEL, OASI (Ticino) and ANU (Graubünden) networks corrected for meteorological variability, PSI Bericht Nr. 08-03, Villigen, Switzerland, 2008.

Kutner, M. H., Nachtsheim, C. J., and Neter, J.:Applied Linear Regression Models, 4th edn, McGraw-Hill, Maidenhead, 2004.

Lanz, V. A., Alfarra, M. R., Baltensperger, U., Buchmann, B., Hueglin, C., and Prévôt, A. S. H.: Source apportionment of submicron organic aerosols at an urban site by factor analytical modelling of aerosol mass spectra, Atmos. Chem. Phys., 7, 1503–1522, doi:10.5194/acp-7-1503-2007, 2007.

Lanz, V. A., Alfarra, M. R., Baltensperger, U., Buchmann, B., Hueglin, C., Szidat, S., Wehrli, M. N., Wacker, L., Weimer, S., Caseiro, A., Puxbaum, H., and Prévôt, A. S. H.: Source attribution of Submicron Organic Aerosols during Wintertime Inversions by Advanced Factor Analysis of Aerosol Mass Spectra, Environ. Sci. Technol., 42, 214–220, 2008.

Lanz, V. A., Prévôt, A. S. H., Alfarra, M. R., Weimer, S., Mohr, C., DeCarlo, P. F., Gianini, M. F. D., Hueglin, C., Schneider, J., Favez, O., D'Anna, B., George, C., and Baltensperger, U.: Characterization of aerosol chemical composition with aerosol mass spectrometry in Central Europe: an overview, Atmos. Chem. Phys., 10, 10453–10471, doi:10.5194/acp-10-10453-2010, 2010.

MeteoSwiss, Mittlere monatliche und jährliche Windrosen: http://www.meteoswiss.admin.ch/web/de/klima/klima_schweiz/tabellen/windrichtung.Par.0019.DownloadFile.tmp/chasseral.pdf, 2010a.

Monks, P. S., Granier, C., Fuzzi, S., Stohl, A., Williams M. L., Akimoto, H., Amann, M., Baklanov, A., Baltensperger, U., Bey, I., Blake, N., Blake, R. S., Carlslaw, K., Cooper, O. R., Dentener, F., Fowler, D., Fragkou, E., Frost, G. J., Generoso, S., Ginoux, P., Grewe, V., Guenther, A., Hansson, H. C., Henne, S., Hjorth, J., Hofzumahaus, A., Huntrieser, H., Isaksen, I. S. A., Jenkin, M. E., Kaiser, J., Kanakidou, M., Klimont, Z., Kulmala, M., Laj, P., Lawrence, M. J., Lee, J. D., Liousse, C., Maione, M., McFiggans, G., Metzger, A., Mieville, A., Moussiopoulos, N., Orlando, J. J., O'Down, C. D., Palmer, P. I., Parish, D. D., Petzold, A., Platt, U., Poeschl, U., Prévôt, A. S. H., Reeves, C. E., Reimann, S., Rudich, Y., Sellegri, K., Steinbrecher, R., Simpson, D., ten Brink, H., Theloke, J., van der Werf, G. R., Vautard, R., Vestreng, V., Vlachokostas, Ch., and von Glasow, R.: Atmospheric Composition Change – global and regional air quality, Atmos. Environ., 43, 5268–5350, 2009.

Montgomery, D. C. and Peck, E. A.: Introduction to Linear Regression Analysis, 4th edn., WileyBlackwell, New York, USA, 2006.

Ordóñez, C., Mathis, H., Furger, M., Henne, S., Hüglin, C., Staehelin, J., and Prévôt, A. S. H.: Changes of daily surface ozone maxima in Switzerland in all seasons from 1992 to 2002 and discussion of summer 2003, Atmos. Chem. Phys., 5, 1187–1203, doi:10.5194/acp-5-1187-2005, 2005.

Prévôt, A. S. H., Staehelin, J., Kok, G. L., Schillawski, R. D., Neininger, B., Staffelbach, D., Neftel, A., Wernli, H., and Dom-

men, J.: The Milan photooxidant plume, J. Geophys. Res., 102, 23375–23388, 1997.

Primas, A., Müller-Platz, C. and Kessler, F. M.: Schweizerische Holzstatistik, Erhebung für das Jahr 2008, Swiss Federal Office of Energy, Bern, Switzerland, 2009.

Pryor, S. C. and Barthelmie, R. J.: PM_{10} in Canada, Sci. Total Environ., 177, 57–71, 1996.

Putaud, J.-P., Raes, F., Van Dingenen, R., Bruegemann, E., Facchini, M.-C., Decesari, S., Fuzzi, S., Gehrig, R., Hueglin, C., Laj, P., Lorbeer, G., Maenhaut, W., Mihalopoulos, N., Mueller, K., Querol, X., Rodriguez, S., Schneider, J., Spindler, G., ten Brink, H., Kjetil, T., and Wiedensholer, A.: A European aerosol phenology–2: chemical characteristics of particulate matter at kerbside, urban, rural and background sites in Europe, Atmos. Environ., 38, 2579–2595, 2004.

R Development Core Team: R: A language and environment for statistical computing. R Foundation for Statistical Computing, Vienna, Austria, http://www.R-project.org., 2008.

Sandradewi, J., Prévôt, A. S. H., Szidat, S., Perron, N., Lanz, V. A., Weingartner, E., and Baltensperger, U.: Using aerosol light absorption measurements for the quantitative determination of wood burning and traffic emission contributions to particulate matter, Environ. Sci. Technol., 42, 3316–3323, 2008.

Schwarz, G.: Estimating the dimensions of a model, Ann. Statist., 6, 461–464, 1978.

Seibert, P., Beyrich, F., Gryning, S.-E., Joffre, S., Rasmussen, A., and Tercier, P.: Review and intercomparison of operational methods for the determination of the mixing height, Atmos. Environ., 34, 1001–1027, 2000.

Spindler, G., Mueller, K., Brueggemann, E., Gnauk, T., and Hermann, H.: Long-term size-segregated characterization of PM_{10}, $PM_{2.5}$ and PM_1 at the IfT research station Melpitz dowinwind of Leipzig (Germany) using high and low-volume filter samplers, Atmos. Environ., 38, 5333–5347, 2004.

Stedman, J. R.: The use of receptor modeling and emission inventory data to explain the downward trend in UK PM_{10} measurements, Atmos. Environ., 36, 4089–4101, 2002.

Stemmler, K., Bugmann, S., Buchmann, B., Reimann, S., and Staehelin, J.: Large decrease of VOC emissions of Switzerland's car fleet during the past decade: results from a highway tunnel study, Atmos. Environ., 39, 1009–1018, 2005.

Swiss Federal Commission for Air Hygiene: Feinstaub in der Schweiz, Status Report of the Swiss Federal Commission for Air Hygiene, Bern, Switzerland, 141 S., available at: http://www.ekl.admin.ch/fileadmin/ekl-dateien/dokumentation/d-bericht-feinstaub-2008.pdf, 2007.

Swiss Federal Council: Luftreinhalte-Verordnung, Swiss Federal Council, Bern, Switzerland, 814.318.142.1, available at: http://www.admin.ch/ch/d/sr/8/814.318.142.1.de.pdf, 2010a.

Swiss Federal Council: Verordnung ueber die technischen Anforderungen an Strassfahrzeuge, Swiss Federal Council, Bern, Switzerland, 741.41, available at: http://www.admin.ch/ch/d/sr/741_41/index.html, 2010b.

Swiss Federal Council: Future of National Infrastructure Networks in Switzerland, Report by the Swiss Federal Council, available at: http://tiny.cc/quydg, 2010c.

Swiss Federal Statistical Office: Multidimensional online database, available at:http://superweb-close.bfs.admin.ch/superweb/logon.jsp?language=en, 2010.

Szidat, S., Prévôt, A. S. H., Sandradewi, J., Alfarra, M. R., Synal, H.-A., Wacker, L., and Baltensperger, U.: Dominant impact of residential wood burning on particulate matter in Alpine valleys during winter, Geophys. Res. Lett., 34, L05820, doi:10.1029/2006GL028325, 2007.

Vardoulakis, S. and Kassomenos, P: Sources and factors affecting PM_{10} levels in two European cities: Implications for local air quality management, Atmos. Environ., 42, 3949–3963, 2008.

Velders, G. J. M. and Matthijsen, J.: Meteorological variability in NO_2 and PM_{10} concentrations in the Netherlands and its relation with EU limit values, Atmos. Environ., 43, 3858–3866, 2009.

Vestreng, V., Myhre, G., Fagerli, H., Reis, S., and Tarrasn, L.: Twenty-five years of continuous sulphur dioxide emission reduction in Europe, Atmos. Chem. Phys., 7, 3663–3681, doi:10.5194/acp-7-3663-2007, 2007.

Vestreng, V., Ntziachristos, L., Semb, A., Reis, S., Isaksen, I. S. A., and Tarrasón, L.: Evolution of NO_x emissions in Europe with focus on road transport control measures, Atmos. Chem. Phys., 9, 1503–1520, doi:10.5194/acp-9-1503-2009, 2009.

Wanner, H. and Hertig, J.-A.: Studies of urban climates and air pollution in Switzerland, J. Clim. App. Meteorol., 23, 1614–1625, 1984.

Wanner, H., Salvisberg, E., Rickli, R., and Schüepp, M.: 50 years of Alpine Weather Statistics (AWS), Meteorologische Zeitschrift, Neue Folge, 7, 99–111, 1998.

Weber, R. O. and Prévôt, A. S. H.: Climatology of ozone transport from the free troposphere into the boundary layer south of the Alps during North Foehn, J. Geophys. Res., 107, 4030, doi:10.1029/2001JD000987, 2002.

Wilks, D. S.: Statistical Methods in the Atmospheric Sciences, 2nd edn., Elsevier, Amsterdam, Netherlands, 2006.

Wood, S. N.: Generalized Additive Models: An Introduction with R. Chapman & Hall/CRC. Boca Raton, USA, ISBN 9781584884743, 2006.

Wood, S. N.: Fast stable direct fitting and smoothness selection for generalized additive models. J. R. Statist. Soc. B, 7, 495-518, 2008.

Zemp, E., Elsasser, S., Schindler, S., Künzli, N., Perruchoud, A. P., Domenighetti, G., Medici, T., Ackermann-Liebrich, U., Leuenberger, P., Monn, C., Bolognini, G., Bongard, J.-P., Brändli, O., Karrer, W., Keller, R., Schöni, M. H., Tschopp, J.-M., Villiger, B., Zellweger, J.-P., and the SAPALDIA Team: Long-Term Ambient Air Pollution and Respiratory Symptoms in Adults (SAPALDIA Study), Am. J. Resp. Crit. Care, 159, 1257–1266, 1999.

Zidek, J., Sun, L., Le, N., and Ozkaynak, H.: Contending with space-time interaction in the spatial prediction of pollution: Vancouver's hourly ambient PM_{10} field, Environmetrics, 13, 595–613, 2002.

Zolghadri, A. and Cazaurang, F.: Adaptive nonlinear state-space modeling for the prediction of daily PM_{10} concentrations, Environ. Modell. Softw., 21, 885–894, 2006.